

# 國立交通大學

理學院應用科技學程

## 碩士論文

互補式金氧半導體光二極體晶片  
葡萄糖與組織胺濃度檢測光學感測系統

An optical bio-sensing system for the determination  
of glucose and histamine based on CMOS photodiode chip

研究生：游秉鈞

指導教授：楊裕雄 教授

中華民國九十七年二月

互補式金氧半導體光二極體晶片

葡萄糖與組織胺濃度檢測光學感測系統

An optical bio-sensing system for the determination of glucose and histamine based on CMOS photodiode chip

研究生：游秉鈞

Student：Ping-chun Yu

指導教授：楊裕雄

Advisor：Yuh-Shyong Yang

國立交通大學

理學院應用科技學程



Submitted to Degree Program of Applied Science and Technology

College of Science

National Chiao Tung University

in partial Fulfillment of the Requirements

for the Degree of

Master

in

Degree Program of Applied Science and Technology

Hsinchu, Taiwan, Republic of China

## 中文摘要

在此研究中，我們經由整合互補式金氧半導體製程所生產的光二極體感應晶片、耦合酵素催化反應，發展出一套生醫感測系統。由於生醫診斷上的重要性，我們選擇了葡萄糖與組織胺做為本系統的測量標的。我們發展的組裝系統所量測得到的葡萄糖與組織胺的 $K_m$ 值分別為 4.9 and 125  $\mu\text{M}$ ，其值與UV/Vis光譜儀所分別測量而得到的值(7.2 and 160  $\mu\text{M}$ )相當接近。我們的系統對於葡萄糖與組織胺的最低量測濃度分別為 1  $\mu\text{M}$  與 10  $\mu\text{M}$ 。再者，我們的系統能測量到葡萄糖與組織胺的濃度線性量測範圍，分別為 1  $\mu\text{M}$  至 5 mM 以及 10 至 80  $\mu\text{M}$ 。兩者的濃度線性量測範圍都小於人體血液中葡萄糖與組織胺正常含量的 2 到 10 倍。經由樣本的稀釋，我們的系統將能夠測量人體血液中的葡萄糖與組織胺的濃度。未來，我們的目標將特別針對多功能家用醫療診斷儀器進行進一步的研究。

## **ABSTRACT**

We developed a biomedical diagnosis system by integrating CMOS photodiode chip and coupled enzyme reactions. Glucose and histamine are the chosen targets because of their importance in the medical diagnosis. The  $K_m$  value of glucose and histamine obtained from our assembled system is 4.9 and 125  $\mu\text{M}$ , respectively, which are similar to those obtained from UV/Vis spectrophotometer (7.2 and 160  $\mu\text{M}$ ). The detection limits of glucose and histamine concentrations in our system are 1  $\mu\text{M}$  and 10  $\mu\text{M}$ , respectively. The linear ranges are from 1  $\mu\text{M}$  to 5 mM and 10 to 80  $\mu\text{M}$  for glucose and histamine, respectively, which both are 2 to 10 folds lower than those in the human blood. In the future, our research will particularly aim at multi-functional household medical diagnosis instrument.



## Acknowledgement

交通大學碩士班的學習在此進入尾聲。回顧兩年多來的歷程，楊教授耐心引導與觀念溝通讓秉鈞受益良多，感謝楊老師的指導。酵素與蛋白質工程實驗室的夥伴們都是秉鈞學習生涯中的良師益友，奇翰、政哲、郝吟、程允、淵仁、陸宜、志衡與漢平，謝謝你們！研究過程中有你們的協同腦力激盪，讓秉鈞學業與心靈上都獲得成長。因為有你們，秉鈞面對研究困境時能夠保持沉著與樂觀。秉鈞還要感謝交通大學電子研究所黃遠東教授與合作夥伴博士研究生張育維。跨領域的研究，需要密切配合與觀念溝通，黃教授與育維對於晶片系統的實驗結果與現象的嚴謹解析，使得研究的成果更加豐碩。甚而，初步研究成果的發表獲得IEEE 2007年EDSSC國際研討會獲選會議論文的肯定。楊教授與黃教授兩位老師的指導，秉鈞與育維十分感恩。台北縣立溪崑國中同事們，佩怡與憲調，兩年來謝謝你們的協助！秉鈞經常在熬夜實驗後仍要面對整天的數學教學，端賴你們每天在上課前叫醒因為體力透支而趴在辦公桌上沉睡的我。還有好友建德與美桂老師，謝謝你們每天的關懷與鼓勵！

好朋友柏如，你的心靈支持與鼓勵，讓我勇往直前面對最後衝刺階段。因為有你，我的生命更臻完美，謝謝你！

最後，秉鈞要將論文獻給我的父母。謝謝你們陪伴我一路走來，始終支持我生命中的每個選擇。由於你們堅定的支持，讓秉鈞在面對挑戰時能夠勇敢積極並堅持到底。二位大菩薩，感恩！

<b>CONTENTS</b>	<b>PAGE</b>
<b>Abstract (Chinese)</b> .....	<b>i</b>
<b>Abstract (English)</b> .....	<b>ii</b>
<b>Acknowledgement</b> .....	<b>iii</b>
<b>Contents</b> .....	<b>iv</b>
<b>Contents of TABLES and FIGURES</b> .....	<b>vi</b>
<b>Abbreviation</b> .....	<b>viii</b>
<b>Chapter 1. Introduction</b>	
<b>1.1 Development progress of optical biosensor</b> .....	<b>1</b>
<b>1.2 The design of CMOS photodiode chip</b> .....	<b>3</b>
<b>1.3 Glucose and histamine determination in medical diagnosis</b> .....	<b>4</b>
<b>1.4 Biochemical reactions</b> .....	<b>5</b>
<b>Chapter 2. Materials and methods</b>	
<b>2.1 Materials</b> .....	<b>8</b>
<b>2.2 Equipments</b> .....	<b>8</b>
<b>2.3 Methods</b> .....	<b>9</b>
<b>Chapter 3. Results</b>	
<b>3.1 CMOS photodiode chip performance</b> .....	<b>19</b>

<b>3.2 Optimization of enzyme assay</b>	<b>20</b>
<b>3.3 The determination of hydrogen dioxide</b>	<b>24</b>
<b>3.4 Coupled enzyme assay to determine <math>\beta</math>-D(+)-glucose and histamine</b>	<b>24</b>
<b>Chapter 4. Discussion</b>	<b>26</b>
<b>Chapter 5. Conclusion</b>	<b>28</b>
<b>Reference</b>	<b>29</b>
<b>Tables and figures</b>	<b>33</b>



**CONTENTS OF TABLES AND FIGURES** **PAGE**

**TABLES**

**TABLE I** The growing problems of diabetes .....33

**TABLE II** Optimal conditions of enzyme reactions .....34

**TABLE III** Enzyme kinetic parameters .....35

**TABLE IV** The feathers of spectrophotometer and the assembled biosensing system .....36

**FIGURES**

**Fig. 1.** The flowchart of research .....37

**Fig. 2.** The flowchart of CMOS optical biosensing system .....38

**Fig. 3.** Top view and cross section of P+/N well finger photodiode .....39

**Fig. 4.** The configuration of subsequent circuits .....40

**Fig. 5(a).** The curve of LED (650nm) input voltage versus light intensity 41

**Fig. 6.** CMOS photodiode light absorptive wavelength scan curve .....43

**Fig. 7.** The absorption light wavelength scan of ABTS / H<sub>2</sub>O<sub>2</sub> colorimetry reaction .....44

**Fig. 8.** The absorption light wavelength scan of the coupled enzyme reactions catalyzing histamine .....45

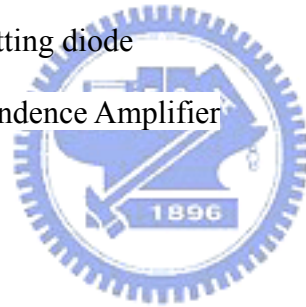
**Fig. 9.** The curve of initial rate versus the different HRP



Concentration .....	46
<b>Fig. 10. The curve of initial rate versus the concentration of ABTS ....</b>	<b>47</b>
<b>Fig. 11. The curve of initial rate versus the different GOx concentration</b>	<b>48</b>
<b>Fig. 12 The curve of initial rate versus the different DAO concentration</b>	<b>49</b>
<b>Fig. 13 The pH profile of <math>\beta</math>-D-(+)-glucose coupled enzyme reactions ..</b>	<b>50</b>
<b>Fig. 14 The pH profile of histmaine coupled enzyme reactions .....</b>	<b>51</b>
<b>Fig. 15 The temperature effect of <math>\beta</math>-D-(+)-glucose coupled enzyme reactions .....</b>	<b>52</b>
<b>Fig. 16 The temperature effect of hitamine coupled enzyme reactions</b>	<b>53</b>
<b>Fig. 17. The CMOS chip output voltage at different hydrogen dioxide concentrations in the 650 nm and 430 nm system. ....</b>	<b>54</b>
<b>Fig. 18. Hydrogen dioxide detection limit in the 650 nm system. ....</b>	<b>55</b>
<b>Fig. 19. Hydrogen dioxide detection limit in the 430 nm system. ....</b>	<b>56</b>
<b>Fig. 20. Hydrogen dioxide linear detection range in the 650 nm system. ..</b>	<b>57</b>
<b>Fig. 21. Hydrogen dioxide linear detection range in the 430 nm system. ..</b>	<b>58</b>
<b>Fig. 22 (a). Enzyme kinetic analysis of glucose oxidase on our assembled biosensor system .....</b>	<b>59</b>
<b>Fig. 23(a). Enzyme kinetic analysis of diamine oxidase on our assembled biosensor system .....</b>	<b>61</b>

## Abbreviation

<b>ABTS</b>	2,2'-azino-bis(3-ethylbenzthiazoline-6-sulphonic acid)
<b>CMOS</b>	Complementary Metal Oxide Semiconductor
<b>DAO</b>	Diamine oxidase
<b>GOx</b>	Glucose Oxidase
<b>GPIB</b>	General Purpose Interface Bus
<b>HRP</b>	Horseradish Peroxidase
<b>LED</b>	Light emitting diode
<b>TIA</b>	Transimpedance Amplifier



## **CHAPETR 1. INTRODUCTION**

Following the progress of the biochip technology in biochemistry and medical diagnosis, the development of an accurate, cost-effective, portable and easy-to-use biosensor system has become the most important issue in the healthcare industry [1–3]. *The early biochips were developed to be used for the measurement of products in enzyme catalyzed reactions e.g. the metabolic species glucose or lactate [4–5]. Now the key principle of biochips is the detection and quantification of affinity binding of molecular complexes, where the transducers mainly use the evaluation of colorimetric or fluorescence signals [6] or electrochemical methods [7–12].*



### ***1.1 Development progress of optical biosensor***

Optical sensors represent a trend recently in biosensor development because of those advantages described above [13]. *In early years, optical biosensors are developed based on optical fiber technology, which is used as a waveguide medium to transmit light signal from the immobilized enzyme to the photomultiplier tube [13–18].* Owing to an expensive set-up, including a photomultiplier tube and associated equipment, the application of the fiber-optic biosensors was limited. To fabricate a miniature optical biosensor, replacing the photomultiplier tube with a photodiode was reported in 1994 [19]. However, its detecting range of hydrogen peroxide was small and the whole system was complicated. An exquisite and miniature photodiode

fabricated by the mature procedure of complementary metal oxide semiconductor (CMOS) technology was integrated in optical biosensor system. With the benefit of low cost, many reports have demonstrated that the CMOS photo sensor is a powerful light detecting device [20 – 22]. Although many CMOS photodiodes had demonstrated for detecting weak light such as luminescence or fluorescence, short lifetime and low light density of light sources are the main barriers in the development of household medical diagnosis instrument.

In our study, we took another approach to achieve the optical biosensor system. Instead of the short lifetime and low light density of bioluminescence and fluorescence, we provided stable light resource by light emitting diode (LED). With the slight variation of light transition power density, the CMOS photodiode detected the colorimetric enzyme catalysis. Following this scheme, we demonstrated a prototype of optical biosensor system with light transition method. In the future, we attempt to develop the miniature system for household medical diagnosis.

The superiorities of our system compared with the PMT system (UV/Vis spectrophotometer) are showed in **TABLE IV**. Our system has several advantages such as low cost, small size and the possibility of array-form development.

## *1.2 The design of CMOS photodiode chip*

We applied the optical sensing theorem by light transition. A novel design of photodiode with finger structure (p+-n well) shortens the distance of electron drift, and increases the area of depletion layer closed to the surface. Therefore, the photodiode receipts carriers more efficiently, and then it could produce higher photosensitive current. When the interval of each bar is twice the width of depletion layer, the photodiode has the best sensitivity. The photocurrent is amplified by a current amplifier, and then the current is translated into an output voltage within 0.49~2.02 V by Transimpedance Amplifier (TIA). Three variable resistances are designed for low light intensity (R1/10 M $\Omega$ ), normal light intensity (R2/1 M $\Omega$ ), and high light intensity (R3/0.1 M $\Omega$ ), separately. Photodiode with finger structure (p+-n well), current amplifier, TIA circuit with variable resistance are designed by Yu-Wei Chang who is a Ph.D. student of the department of electronic engineering at NCTU.

### **Our study**

In our study, we set up a CMOS chip prototype biosensor system to quantify the glucose and histamine in the reagent. And we demonstrate that the detection range of the system matched with the amount of glucose and histamine in human body. Integrating with the development of the micro array system and user interface, the miniature instrument for biomedical research and household medical diagnosis can be

realized in the future.

### ***1.3 Glucose and histamine determination in medical diagnosis***

#### **Glucose**

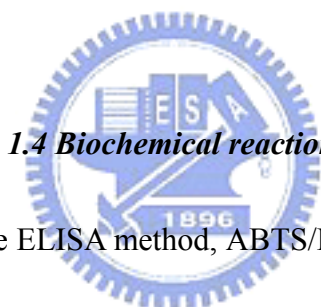
It is estimated that there are over 170 million diabetics worldwide (WHO, 2004). This is projected to increase to 366 million by 2030 (WHO, 2006). It still gets worse that incidence of the disease has risen by an alarming 11% over the last 5 years, and a further doubling of new cases is predicted in the next 25 years. **TABLE 1** illustrates the statistics of the growing global diabetes problem.

*Despite the many technological advances in research and development of biosensor and the introduction of many different products, glucose biosensors still account for approximately 85% of the current world market for biosensors, which has recently been estimated to be around \$5 billion [23]. The greatest reason why the glucose biosensor market is growing in developed nations is the prevalence of diabetes [24]. Therefore, investigating the amount of histamine in human blood is a trend issue in the medical diagnosis.*

#### **histamine**

*Histamine is likely to play an important role in functions involving receptors such*

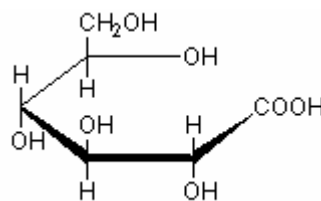
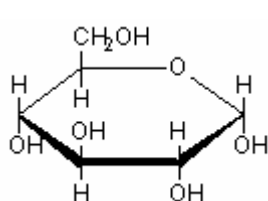
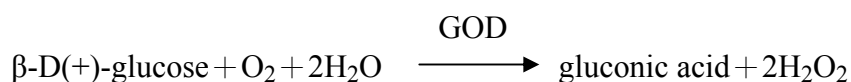
as arousal and the circadian rhythm of food intake and hormone release [25]. A role for the neuronal histamine system as a danger response system is proposed. Considerable evidence suggests that histamine is involved in the response to dangerous situations [26]. On the other hand, histamine is an important chemical involved in many allergic reactions. And it causes several allergic symptoms: (1) inflammatory responses (2) constriction of smooth muscle (asthma). Therefore, investigating the amount of histamine in human blood or foods would be a trend issue in the medical diagnosis and biomedical research.



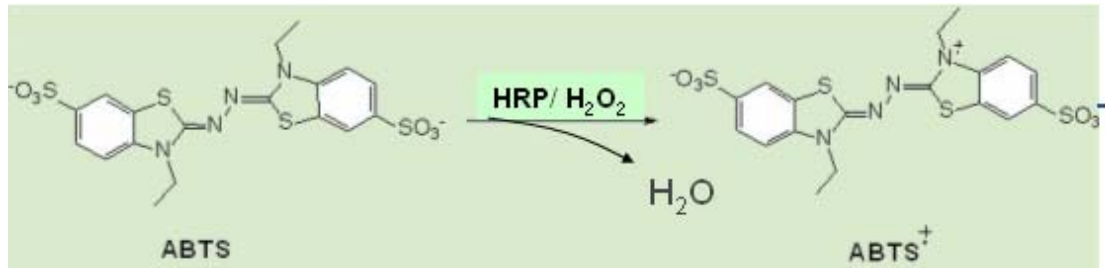
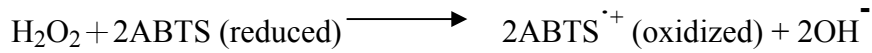
#### 1.4 Biochemical reactions

In our study, we choose the ELISA method, ABTS/H<sub>2</sub>O<sub>2</sub> colorimetric system [33–34] as platform to couple with glucose oxidase and diamine oxidase to determine the amount of free β- D(+)-glucose and histamine. Below are the couple enzyme reactions:

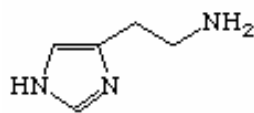
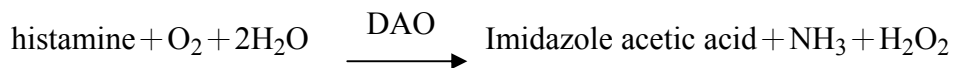
##### Glucose determination reactions



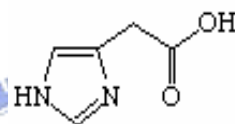
HRP



### *Histamine determination reactions*



Histamine



Imidazole acetic acid



where ABTS represents 2,2'-azino-bis[3-ethylbenzthiazoline-6-sulphonic acid], and

HRP stands for horseradish peroxidase. Since the ABTS solution is visually light

green and the  $\text{ABTS}^+$  solution is dark blue, this chemical reaction can be easily

observed for qualitative analysis. Comparatively, detecting the optical absorbance of

the biochemical material is more accurate for quantitative analysis. The absorbance

(A) of the materials is described by the Beer-Lambert law as

$$A = \log \left( \frac{I_0}{I_1} \right) = \epsilon_\lambda \cdot l \cdot c,$$

where  $I_0$  is the initial light intensity,  $I_1$  is the light intensity after passing through the



material,  $\epsilon\lambda$  is the wavelength-dependent molar absorptivity in units of  $\text{l}\cdot\text{mol}^{-1}\cdot\text{cm}^{-1}$ ,  $l$  is the path length in units of cm, and  $c$  is the concentration of analyte in units of  $\text{mol}\cdot\text{l}^{-1}$  [32]. With a monochromatic light source, the absorbance is proportional to the concentration. Thereby detecting the optical signals modulated by the biochemical reactions is an efficient way to quantities the amount of  $\text{H}_2\text{O}_2$ .

The ELISA method, the system based on ABTS/ $\text{H}_2\text{O}_2$  colorimetric analysis, could be coupled with various enzymes to assay various kinds of substrates. Before analyzing the kinetics of glucose oxidase and diamine oxidase, condition-optimized studies were performed for each of the components of glucose and histamine assay on UV/Vis spectrophotometer (UV-3310, Hitachi). Comparing the kinetics of glucose oxidase and diamine oxidase obtained from UV-3310 and our CMOS device, we could confirm the usability of our assembled biomedical sensor system.

## **CHAPTER 2. MATERIALS AND METHODS**

### ***2.1 Materials***

$\beta$ -D(+)-glucose, horseradish peroxidase (HRP), histamine, diamine oxidase (from porcine kidney)(DAO), 2,2'-azino-bis(3-ethylbenzthiazoline-6-sulphonic acid) (ABTS), and H<sub>2</sub>O<sub>2</sub> (30%, W/W) are purchased from Sigma. Glucose oxidase (from *Aspergillus niger*) (GOx) is purchased from Fluka. Sodium phosphate powders (monobasic and dibasic) are obtained from J. T. Baker.

### ***2.2 Equipments***

Photodiode with finger structure (p+-n well), current amplifier, TIA circuit with variable resistance are designed by Yu-Wei Chang who is a Ph.D. student of the department of electronic engineering at NCTU. And the device was manufactured by CMOS fabrication in TSMC co. Breadboard of red and violet light emitting diodes (LED) are needed to assemble biomedical sensing system which is also composed of quartz cuvette and band-pass color filters. Band-pass color filters have two forms which are 650 nm and 430 nm.

E3646A power supply (Agilent), 4401A multi-meter (Agilent), General Purpose Interface Bus (GPIB) card, and a analysis computer software (Labview 6.0) are used to collect the data output from photodiode chip. UV/vis spectrophotometer (UV-3310,

Hitachi) is used to confirm the validity of the data of our assembled biomedical sensing system.

## **2.3 Methods**

### **Research scheme**

In order to build up a biomedical sensor system, we assembled four main components: optimal conditions of bio-reactions, CMOS chip consist of photodiode and circuit, optical devices, and data process software, is considered reasonably as usual. **Fig. 1** is the flowchart of our research.



### **Reagents preparation**

#### **Sodium phosphate buffer (0.1 M stock)**

0.1 M dibasic phosphate solution was prepared by add ddH<sub>2</sub>O to 7.1 g Na<sub>2</sub>HPO<sub>4</sub> until final volume 500 ml was obtained. 0.1 M monobasic phosphate solution was prepared by add ddH<sub>2</sub>O to 6.9g NaH<sub>2</sub>PO<sub>4</sub> · H<sub>2</sub>O until final volume 500 ml was obtained. Then added NaH<sub>2</sub>PO<sub>4</sub> solution to Na<sub>2</sub>HPO<sub>4</sub> solution until the desired pH 7.0 was obtained. Phosphate buffer was stored at room temperature.

#### **ABTS (2,2'-azino-bis(3-ethylbenzthiazoline-6-sulphonic acid) / 36 mM stock)**

36mM ABTS solution was prepared by add phosphate buffer to 9 tabs ABTS (10

mg/tab) until final volume 4.556 ml was obtained. And then add NaOH to ABTS solution until the desired pH 7.0 was obtained. ABTS solution had to be prepared fresh and keep it from light lest it would go off.

### **H<sub>2</sub>O<sub>2</sub> (1M stock)**

Added ddH<sub>2</sub>O to 1ml H<sub>2</sub>O<sub>2</sub> (30%, W/W) until final volume 9 ml was obtained. And then, we diluted this stock with ddH<sub>2</sub>O to obtained 0.1M and 0.01 M solution.

### **Glucose solution (1 M stock)**

Glucose solution was prepared by adding ddH<sub>2</sub>O to dissolve 9 mg glucose powder until final volume 50ml was obtained. And then, we diluted this stock with ddH<sub>2</sub>O to obtained 0.1 M and 0.01 M solution.



### **Histamine solution (0.2 M stock)**

Histamine solution was prepared by adding phosphate buffer to dissolve 222 mg histamine powder until final volume 10ml was obtained. And then, we diluted this stock with dd H<sub>2</sub>O to obtained 20mM and 2mM solution.

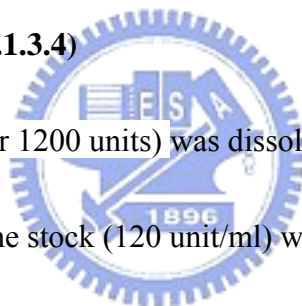
## **Enzyme preparation**

### **Horseradish peroxidase (HRP, EC 1.11.1.7)**

The powder of HRP (4mg or 1000 units) was dissolved in 10ml sodium phosphate buffer (0.1 M at pH 7.0), and the stock (100 unit/ml) was stored at  $-80^{\circ}\text{C}$ . One unit of HRP will form 1.0 mg of purpurogallin from pyrogallol in 20 seconds at pH 6.0 at  $20^{\circ}\text{C}$ . This purpurogallin (20 seconds) unit is equivalent to approximately  $18\ \mu\text{M}$  units per minute at  $25^{\circ}\text{C}$ .

### **Glucose oxidase (GOx, EC 1.1.3.4)**

The powder of GOx (6mg or 1200 units) was dissolved in 10ml sodium phosphate buffer (0.1 M at pH7.0), and the stock (120 unit/ml) was stored at  $-80^{\circ}\text{C}$ . One unit corresponds to the amount of enzyme which oxidizes  $1\ \mu\text{mol}$  glucose per minute at pH 7.0 and  $25^{\circ}\text{C}$ .



### **Diamine oxidase (DAO, EC 1.4.3.6)**

The powder of DAO (200mg or 10 units) was dissolved in 1ml sodium phosphate buffer (0.1 M at pH7.0), and the stock (10 unit/ml) was stored at  $-80^{\circ}\text{C}$ . One unit will oxidize  $1.0\ \mu\text{mole}$  of putrescine per hour at pH 7.2 and  $37^{\circ}\text{C}$ .

## **Optimal condition for enzyme assay**

### **Absorption wavelength of product**

The “wavelength scan” function of UV-3310 was used to measure the range of absorption wavelength of reaction product. The scan parameters of UV-3310 are as follows: start wavelength is 700 nm, end wavelength is 300 nm, delay time is 120 sec, scan speed is 300 nm/min and slit is 2 nm. Reaction condition is: 25°C, pH 7.0, 100 mM phosphate buffer, 30 mM ABTS, 0.2 mM H<sub>2</sub>O<sub>2</sub> and 0.2 unit/ml HRP.

### **Optimal concentration of reagents**

Optimization of substrate amount (H<sub>2</sub>O<sub>2</sub>, glucose, and histamine) played an important role in enzyme assay before the determination in the solution. The “time scan” function of UV-3310 was used to find out the optimal concentration of reagents.

The scan parameters of UV-3310 were: wavelength is 430nm (H<sub>2</sub>O<sub>2</sub> / histamine) and 650nm (H<sub>2</sub>O<sub>2</sub> / glucose), sampling interval is 1 sec; total times are 60 sec for H<sub>2</sub>O<sub>2</sub>, 120sec for glucose, and 1200sec for histamine, and delay time is zero. Several reaction conditions were kept under 25°C (H<sub>2</sub>O<sub>2</sub> and glucose) and 37°C (histamine), pH 7.0, 100 mM phosphate buffer.

The optimization studies began with ABTS/H<sub>2</sub>O<sub>2</sub> colorimetric system to find out the linear range of HRP, and then appropriate amount of HRP, excess ABTS, were

added to Fig. out the optimal concentration of reagents. After finding out the suitable amount of other reagents, we coupled ABTS/H<sub>2</sub>O<sub>2</sub> colorimetric system with glucose oxidation reaction to find out the linear range of glucose oxidase (650 nm). Repeating previous process, we also found out the linear range of diamine oxidase (430 nm).

### **Optimal pH value of buffer**

The “time scan” function of UV-3310 was used to find out the optimal pH value of phosphate buffer. In the experiment of glucose, value of pH ranged from 3.0 to 9.0 with an interval of 1.0 and three kinds of buffer system, citrate buffer (pH 3.0~5.0), phosphate buffer (pH 5.0~6.0), Tris buffer (pH 7.0~9.0) were used. The scan parameters of UV-3310 are: wavelength is 650 nm, sampling interval is 1 sec, total time is 120 sec, and delay time is zero. Constant reaction conditions were: 25°C, 30 mM ABTS, 20 mM glucose, 0.48unit/ml GOD and 0.2 unit/ml HRP. For determine histamine, value of pH range is from 6.5 to 7.5 with an interval of 0.5 and phosphate buffer (pH 6.5~7.5), was used. The scan parameters of UV-3310 are: wavelength is 430 nm, sampling interval is 1 sec, total time is 1200 sec, and delay time is zero. Constant reaction condition is: 37°C, 30 mM ABTS, 2 mM histamine, 0.8 unit/ml DAO and 0.2 unit/ml HRP.

### **Optimal temperature**

The “time scan” function of UV-3310 was used to find out the optimal temperature for the coupled enzyme assay. Temperature ranges from 20°C to 40°C. All reagents except enzymes were mixed, and then enzymes were added into mixed reagents immediately before we began to measure the process of time scan. The scan parameters of UV-3310 were: wavelength is 650 nm (glucose), 430 nm (histamine), sampling interval is 1 sec, total times are 120 sec (glucose), 1200 sec (histamine) and delay time is zero. Constant reaction condition is: pH 7.0, 30 mM ABTS, 20 mM Glucose/ 2 mM Histamine, 0.48 unit/ml GOD / 0.8 unit/ml DAO, and 0.2 unit/ml HRP.



### **Coupled enzyme assay to determine concentration of substrate**

#### **Glucose determination**

ABTS/H<sub>2</sub>O<sub>2</sub> colorimetric system coupled to GOD catalyzed reaction could determine the concentration of glucose. The reaction conditions for this coupled enzymes system contained 0.48 unit/ml GOD, 0.2 unit/ml HRP, 30 mM ABTS and phosphate buffer (100 mM, pH 7.0) in a final volume of 1 ml at 25°C.



## Histamine determination

ABTS/H<sub>2</sub>O<sub>2</sub> colorimetric system coupled to DAO catalyzed reaction can determine the concentration of histamine. The reaction conditions for this coupled enzymes system contained 0.8 unit/ml DAO, 0.2 unit/ml HRP, 30Mm ABTS and phosphate buffer (100 mM, pH 7.0) in a final volume of 1 ml at 37°C.

## Mixing procedure

*Aliquot amount of enzyme is added into the cuvette following by the injection of all other necessary reagents and sample. These processes are to make sure that the whole compounds are well mixed in cuvette without extra shaking and the data can be collected in a short period of time [20].*



## Data processing

Each data point was calculated from the mean value of triplicate assay. The curve and  $K_m$  value were obtained with Michaelis-Menten equation in enzyme kinetics analysis of Sigma Plot 2001.

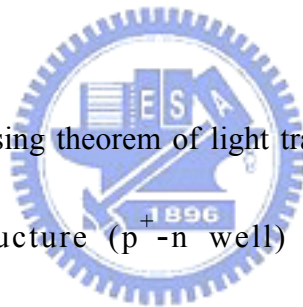
## CMOS chip design and biomedical sensor system setup

The flowchart of the proposed CMOS optical biosensing system is illustrated in **Fig.**

2. A narrowband LED was used as the light source, and a bandpass filter allowed the light of a specific wavelength to travel through the cuvette, in which the light was modulated by the biochemical materials. The light, after passing through the cuvette, was detected by the CMOS biochip. The CMOS photo detector converted the modulated optical signals into current signals, and then the transimpedance amplifier (TIA) converted them into voltage signals. Finally, the signals were recorded by a multimeter and processed by personal computer.

### CMOS photodiode

We applied the optical sensing theorem of light transition. And a novel design of photodiode with finger structure ( $p^+ - n$  well) shortened the distance of electron drift, and increased the area of depletion layer closed to the surface. Therefore, the photodiode received carriers more efficiently, and then it could produce higher photosensitive current. When the interval of each bar is the twice width of depletion layer, the photodiode has the best sensitivity. The CMOS biochip is mainly composed of a photo detector and a TIA. **Fig. 3** illustrates the top view and cross section of the proposed  $P^+/N$ well finger photodiode. The quantum efficiency of the photodiode is enhanced by adopting interdigitated shallow  $P^+/N$ well junctions to extend the depletion regions



[27]. Each P+ stripe is  $1\mu\text{m}$  wide with  $4\mu\text{m}$  spacing, and the total area of this finger photodiode is  $100\mu\text{m} \times 100\mu\text{m}$ . The photodiode is surrounded by double guard rings to keep the substrate noise off; the P+ guard ring is connected to ground, and the N+ guard ring is connected to a high potential [28]. Photodiode with finger structure (p+-n well), current amplifier, TIA circuit with variable resistance are designed by Yu-Wei Chang who is a Ph.D. student of the department of electronic engineering at NCTU.

### **Circuit design**

As shown in **Fig. 4**, the subsequent circuits include a current source, current mirrors, a TIA, and output buffers. The TIA consists of a common-source stage (M0), two source followers (M1 and M2), and an external feedback resistance (RF). M1 serves in the feedback loop to isolate R0 from the loading effect, and M2 drives the load capacitance to alleviate the stability issue [29].

### **Light source module**

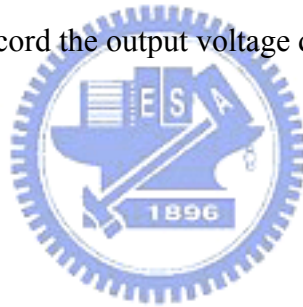
We choose two high lightness red LED and a color filter with 650nm to form a light source module, and select  $R2/1\text{ M}\Omega$  (normal light intensity) on TIA. With preceding setup, we determined glucose amount in the reagent. On the other hand,

we choose three high lightness violet LED and a color filter with 430 nm to form a light source module, and select R1/10 M $\Omega$  (low light intensity) on TIA.

### **Data analysis**

Data analysis consists of hardware and software; therefore, we have to connect them with our biomedical sensor system. E3646A power supply provides CMOS chip 3.0 V bias voltage, and 4401A multimeter collects the output voltage data and transfers it to a personal computer (PC) through GPIB connection.

And we use Labview 6.0 to record the output voltage data transferred to PC.



## CHAPETR 3. RESULTS

### *3.1 CMOS photodiode chip performance*

The biochip is implemented in a standard 0.35- $\mu\text{m}$  CMOS technology. The finger photodiode is reverse-biased moderately to ensure that the photocurrent is proportional to the absorbed photons. The photocurrent is then converted into voltage signals by the subsequent TIA. With a 3.0 V power supply, the lower bound and upper bound of the output voltage are 0.49 V and 2.02 V, respectively. (See **Fig. 5 (a)–(c)**) Therefore, we obtained a linear range of output voltage to compare with the input light intensity which was proportioned to the concentration of  $-D(+)$ -glucose or histamine.



#### **Circuit design**

When photodiode absorbs photons, it will generate a flow of current in an external circuit, proportional to the incident light. The photocurrent was amplified by current amplifier, and then the current was translated into voltage output within 0.49~2.02 V by Transimpedance Amplifier (TIA). The circuit design is showed in **Fig. 4**. Three variable resistances were designed for low light intensity ( $R1/10\text{ M}\Omega$ ), normal light intensity ( $R2/1\text{ M}\Omega$ ), and high light intensity ( $R3/0.1\text{ M}\Omega$ ).

Before we know the corresponding concentration of reagents by measuring the

voltage value, the liner relation between light intensity and output voltage of CMOS chip must be confirmed. To affirm this, the first step, the module of LED was gave various input voltages, and a color filter was used to sift the specific-wavelength light out. In the meanwhile, the corresponding values of light intensity were measured by power meter. Then we could build up a curve of LED input voltage versus light intensity such as **Fig. 5(a)**. The second step, we gave various LED input voltages as serious light intensity, and measure the corresponding output voltages of CMOS chip. Then we could also build up another curve of LED input voltages versus CMOS chip output voltage such as **Fig. 5(b)**. The third step, with merging two curves previously, we get a new curve of light intensity versus CMOS chip output voltage. It is showed as **Fig. 5(c)**. According to the linear relation showed as **Fig. 5(c)**, we can translate the CMOS chip output voltage collected by 4401A multimeter into transiting light intensity.

### ***3.2 Optimization of enzyme assay***

#### **Absorption wavelength of product in glucose and histamine oxidation reaction**

It illustrates the absorption peak of photodiode between 400 and 1000 nm, and it is obvious that the maximum absorption peak of photodiode within the visible light ranges between 600 and 700nm. Furthermore, it shows that the absorption sepctrum

of the product of reaction,  $\text{ABTS}^{\cdot+}$ , and it has three absorption peaks at 415 nm, 640 nm and 720 nm, separately (**Fig. 7**). Light 1 in **Fig. 6** reveals the weaker absorption peak of photodiode and Light 2 shows the stronger one. After all we will confirm that our photodiode could have the corresponding performance and it could also determine the glucose amount in the reagent. Therefore, we choose 650 nm as the optimal absorptive wavelength in the glucose oxidation reaction.

On the other hand, we want to confirm that the performance of our photodiode could fit the optimal light absorbance peak of  $\text{ABTS}/\text{H}_2\text{O}_2$  colorimetry system with the range from 390 nm to 440 nm. As a matter of fact, the product of coupled enzyme reactions catalyzing histamine had only one light absorbance peak at 430 nm (**Fig. 8**). Therefore, we choose 430 nm as the optimal absorption wavelength of histamine oxidation reaction.

## **Optimal concentration of reagents**

### **$\text{ABTS}/\text{H}_2\text{O}_2$ colorimetry system**

There is a linear range of HRP between 0.05 to 0.2 U/ml (**Fig. 9**); therefore, we choose 0.2 U/ml of HRP to catalyze in the  $\text{ABTS}/\text{H}_2\text{O}_2$  colorimetry system. We added excess  $\text{H}_2\text{O}_2$  in  $\text{ABTS}/\text{H}_2\text{O}_2$  colorimetry system with various concentrations of ABTS to investigate the optimal concentration of ABTS. In the consideration of the

solubility of ABTS and the catalytic rate in **Fig. 10**, we choose 30 mM to be the optimal concentration of ABTS to make sure of its continuous working.

### **Determination of optimal amount of glucose oxidase and diamine oxidase**

After we found out the optimal concentration of other reagents, we coupled ABTS/H<sub>2</sub>O<sub>2</sub> colorimetry system with glucose oxidation reaction to find out the linear range of glucose oxidase ranged from 0.01 to 0.8 U/ml as shown in **Fig. 11**. Therefore, we choose appropriate amount, 0.48 U/ml, of glucose oxidase to catalyze glucose oxidation reaction. Additionally, we coupled ABTS/H<sub>2</sub>O<sub>2</sub> colorimetry system with histamine oxidation reaction to find out the linear range of diamine oxidase ranged from 0.4 to 2 U/ml as shown in **Fig. 12**. Therefore, we choose appropriate amount, 0.8 U/ml, of diamine oxidase to catalyze histamine oxidation reaction.

### **Optimal pH value of phosphate buffer**

**Fig. 13** demonstrates that the effect of pH value (3.0, 4.0, 5.0, 6.0, 7.0, 8.0, and 9.0) on the assay. In order to fit the application in biomedical diagnosis, we choose appropriate pH 7.0 to be the optimal pH condition in glucose oxidation reaction. In the side of histamine oxidation reaction, owing to the enzyme activity limitation, we choose the range between 6.5~7.5 to find out optimal pH value according to the



suggestion of sigma enzyme product data sheet. **Fig. 14** tells us that the effect of pH value (6.6, 6.8, 7.0, 7.2, and 7.4) on assay. Base on the result of this experiment, the initial rate in pH value of 7.4 is optimal. Considering these two optimal pH value as described above, we choose a pH 7.0 phosphate buffer for coupled enzyme assay.

### **Optimal temperature**

The relationship between different temperatures ( $20^{\circ}\text{C}\sim 40^{\circ}\text{C}$ ) and initial rates of glucose assay shows as **Fig.15**, it tells us the variation of temperature affect unobviously the catalysis rate of glucose oxidase. On the other hand, there is no temperature controlled setup on our assembled biosensor system. While proceeding any experiment on UV/Vis spectrometer U-3310,  $25^{\circ}\text{C}$  is choose to be the optimal temperature.

Different from glucose oxidation reaction, the variation of temperature does affect the catalysis rate of diamine oxidase obviously. The relationship between different temperatures ( $20^{\circ}\text{C}\sim 40^{\circ}\text{C}$ ) and initial rates of diamine oxidase assay shows as **Fig. 16**, and it tells us initial rates of diamine oxidase has higher value between  $36^{\circ}\text{C}$  and  $40^{\circ}\text{C}$  than on room temperature. Considering the temperature of human body, we choose  $37^{\circ}\text{C}$  as the optimal temperature of histamine oxidation reaction.

### ***3.3 The determination of hydrogen dioxide***

The CMOS chip output voltage at different hydrogen dioxide concentrations in the 650 nm and 430 nm systems were showed in **Fig. 17(a) and Fig. 17(b)**. The hydrogen dioxide detection limit of assembled system in the 650 nm and 430 nm were 1  $\mu\text{M}$  and almost were the same as that from UV/Vis spectrophotometer (shown in Fig. 18(a)-(b) and Fig. 19(a)-(b)). The liner detection ranges of our assembled biosensing system and UV/Vis spectrophotometer ranges from 1 ~ 20  $\mu\text{M}$  and 10 ~ 80  $\mu\text{M}$ , respectively(shown in **Fig. 20 (a)-(b) and Fig. 21 (a)-(b)** ).

### ***3.4 Coupled enzyme assay to determine $\beta$ -D(+)-glucose and histamine***

Coupling glucose oxidase and diamine oxiadse catalyzed reaction with ABTS/H<sub>2</sub>O<sub>2</sub> colorimetry system, we get the enzyme kinetic analysis of  $\beta$ -D(+)-glucose and histamine standard curves. All the curve and  $K_m$  value are obtained with Michaelis-Menten equation in enzyme kinetics analysis of Sigma Plot 2001.

Enzyme kinetic analysis of glucose oxidase and diamine oxidase observed in our assembled biosensor system is shown in **Fig. 22(a) and Fig. 23(a)**. By this process the  $K_m$  value of  $\beta$ -D(+)-glucose and histamine were  $4.9 \pm 0.5 \mu\text{M}$  and  $125 \pm 3.21 \mu\text{M}$ , respectively, which approached to those obtained from UV/Vis spectrophotometer

( $7.2 \pm 0.2 \mu\text{M}$  and  $160 \pm 19.7 \mu\text{M}$  ). (See **TABLE 3(a)**, **TABLE3(b)**, **Fig. 22(b)** and **23(b)**) The optimal reaction conditions of these two enzyme was showed in **TABLE 2**, and the CMOS chip output voltage at different glucose and histamine concentrations were showed in **Fig. 22(c)** and **Fig. 23(c)**.  $\beta$ -D(+)-glucose detection limit of assembled system is  $1 \mu\text{M}$  and almost the same as that from UV/Vis spectrophotometer. On the other hand, the histamine detection limit of assembled system is  $10 \mu\text{M}$  while the hitamine detection limit of UV-vis spectrophotometer is  $20 \mu\text{M}$ . The liner detection ranges of our assembled biosensing system ranges from  $1 \mu\text{M}$  to  $5 \text{mM}$  and  $10 \sim 80 \mu\text{M}$ , respectively.



## **CHAPTER 4. DISCUSSION**

### ***Optimal absorptive wavelength***

There are two factors to determine the optimal absorptive wavelength  $\beta$ -D(+)-glucose and histamine oxidation reactions: The absorption wavelength of the products of  $\beta$ -D(+)-glucose and histamine oxidation reactions; and the absorption peak of CMOS photodiode chip. Owing to the maximum absorption peak of CMOS photodiode chip located between 600 and 700 nm and the absorption peaks of  $\beta$ -D(+)-glucose oxidation reaction were at 415 nm, 650 nm and 720 nm, the 650 nm was chosen to be the optimal wavelength to prove the feasibility of our CMOS photodiode chip. On the other hand, the absorption peak of histamine oxidation reaction was only at 430 nm. Therefore, we follow the normal biochemical rule: Chose the maximum absorption peak of reaction. As matter of fact, the only absorption peak of histamine oxidation reaction was at 430 nm based on the results of our experiment. Although 430nm might not the suitable range of the absorption peak of CMOS photodiode chip, we still wondered whether our CMOS photodiode chip could determinate histamine at 430 nm. Finally, we choose 650 nm and 430 nm to be the optimal absorptive wavelength of glucose and histamine oxidation reactions, respectively.

### *The performance of assembled biomedical system*

Enzyme kinetic analysis results of glucose oxidase and diamine oxidase observed in our assembled biosensor system approached to that obtained from UV/Vis spectrophotometer. Our system was more superior than the traditional optical spectrophotometer whether volume or cost. In the meanwhile, the detection linear ranges of  $\beta$ -D(+)-glucose and histamine obtained from our assembled system approached to the amount in human body. When we determine the  $\beta$ -D(+)-glucose and histamine. The liner detection ranges of our assembled biosensing system ranged from 1  $\mu$ M to 5 mM and 10 ~ 80  $\mu$ M, respectively, while the glucose concentration of human blood is 4 ~ 8 mM [30] and 1~8 mg/dl (90~720  $\mu$ M) [31]. By the 2 to 10 folds sample dilution at most, the detection linear range of our assembled system can determine  $\beta$ -D(+)-glucose and histamine concentration in the human blood.

## CHAPETR 5. CONCLUSION

We have set up an optical bio-sensing system for determination of glucose and histamine. A photodiode chip based on CMOS manufacture procedure was developed with the P+/Nwell finger structure and the subsequent current amplifier circuits, especially, include current mirrors and TIA. The photodiode with the P+/Nwell finger structure is surrounded by double guard rings to keep the substrate noise off. The optical transition theorem is used to be the detection method in our system. We designed colorimetical reactions to be a biochemistry detection platform. Using the platform technology, we can determinate  $\beta$ -D(+)-glucose and histamine in the reagents. The performance of our system can compare with traditional large-size optical instrument, spectrophotometer. And our system has several advantages such as low cost, small size and the possibility of array-form development. In the future, we will aim to developing a new generation system based on this prototype system. Minimization, array, user interface and micro-fluid channel would be integrated with the technology of the prototype system. Our hope is to set up a multi-functional household medical diagnosis instrument. And then, the research integrated with biochemistry and electronic engineering could benefit more people who need house medical care.

## REFERENCES

1. Baeumner, A. J., Cohen, R. N., Miksic V., Min, J., 2003. *Biosens. Bioelectron.* **18**: 405–413
2. Choi, S. H., Gu, M. B., 2002. *Biosens. Bioelectron.* **17**: 433–440
3. DeBusschere, B. D., Kovacs, G. T., 2001. *Biosens. Bioelectron.* **16**: 543–556
4. Wollenberger U., Hintsche, Scheller R. F., 1995. Biosensors for analytical microsystems. In: (ed. Reichl H) *Microsystem technologies*: 687–693
5. Hintsche R., Dransfeld I., Scheller F., Pham M. T., Hoffmann W., Huller J., Moritz W., 1990. *Biosens. Bioelectron.* **5**: 327–334
6. Vo-Dinh T., Cullum B., 2000. Fresenius' *J. Anal. Chem.* **366**: 540–551
7. Palecek E., Fojta M., Jelen F., 2002. *Bioelectrochemistry* **56**: 85–90
8. Wang J., 1999. *Anal. Chem.* **71**: 328–332
9. Kelley S. O., Boon E. M., Barton J. K., Jackson N. M., Hill M. G., 1999. *Nucleic Acids Res.* **27**: 4830–4837
10. Berggren C, Stalhandske P, Brundell J, Johansson G, 1999. *Electroanalysis* **11**: 156–160
11. Alfonta L, Singh A. K. , Willner I. , 2001. *Anal. Chem.* **73**: 91–102
12. Willner I, Willner B, Katz E, 2002. *Rev. Mol. Biotechnol.* **82**: 301–463
13. Ho W. J., Chen J. S., Ker M. D., Wu T. K., Wu C. Y., Yang Y. S., Li Y. K.,

- Yuan C. J., 2007. *Biosens. and Bioelectron.* **22**: 3008–3013.
14. Blum L. J., Gautier S. M., 1991. (eds. Blum L. J., Coulet P. R., Marcel Dekker), *New York*: 213–247
15. Golden J. P., Anderson G. P., Rabbany S.Y., Ligler F. S., 1994. *IEEE Trans. Biomed. Eng.* **41**: 585–591
16. Chen Z., Kaplan D. L., Gao H., Kumar, J., Marx K. A., Tripathy S.K., 1996. *Mater. Sci. Eng. C* **4**: 155–159
17. Marquette C.A., Blum L.J., 1999. *Anal. Chim. Acta.* **381**: 1–6
18. Tsafack V.C., Marquette C.A., Pizzolato F., Blum L., 2000. *Biosens. Bioelectron.* **15**: 125–133
19. Preuschoff F., Spohn U., Janasek D., Weber E., 1994. *Biosens. Bioelectron.* **9**: 281–295
20. Lu U., Hu B. C., Shih Y. C., Wu C. Y., Yang Y. S., 2004. *Biosens. Bioelectron.* **19**: 1185–1191
21. Lu U., Hu B. C.P., Shih Y. C., Yang Y.S., Wu C. Y., Yuan C. J., Ker M. D., Wu T. K., Li Y. K., Hsieh Y. Z., Hsu W., Lin C. T., 2003. *IEEE Sens. J.* **3**: 310–316
22. Huang S. H., Shih Y. C., Wu C. Y., Yuan C. J., Yang Y. S., Li Y. K., Wu T. K., 2004. *Biosens. Bioelectron.* **19**: 1627–1633
23. Newman J. D., Warner P. J., Turner A. P. F., Tigwell L. J., 2004. *Biosensors: A*



*Clearer View*. Cranfield University, UK: 216

24. Newman J. D., Anthony P., Turner F., 2005. *Biosen. Bioelectro.* **20**: 2435–2453
25. Wada H., Inagaki N., Yamatodani A., Watanabe T., 1991. *Trends Neurosci.* **14**: 415–418
26. Ritchie E. Brown, David R. Stevens, Helmut L. Haas, 2001. *Progress in Neurobiology* **63**: 637–672
27. Ghazi A., Zimmermann H., Seegebrecht P., 2002. *IEEE Trans. Electron Devices* **49**: 1124-1128
28. Ker M. D., Lo W. Y., 2003. *IEEE Trans. Semicond. Manuf.* **16**: 319-334
29. Razavi B., *Design of Integrated Circuits for Optical Communications*, McGraw-Hill, 2003.
30. Mackay E. M., *J. Biol. Chem.*, May 27, 1932: 685-689
31. Lubschez R., *J. Biol. Chem.*, September 24, 1949: 731-738
32. Eienthal R. and Danson M. J., 2002, *Enzyme Assays*, 2nd Ed., Oxford University Press.
33. Kunst A., Draeger B., Ziegenhorn J., 1984, *Methods of Enzymatic Analysis* (ed. HU Bergmeyer, Verlag chemie, Weihenheim): 163-172
34. Putter J. and Becker R., 1983, Peroxidase. In “*Method of Enzymatic Analysis*,

*Third Edition 3*” (ed. Bergmeyer, H.U., Verlag chemie, Weihenheim): 286-292



## **TABLES AND FIGURES**

**TABLE I**

The growing global problem of diabetes

Statistics	1995	2000 (estimate)	2025 (estimate)
People with diabetes (million)	135	154	300
% in developed countries	25.2	23.8	17.1
Female/male ratio	1.18	1.16	1.12

Source: World Health Organisation.

It still gets worse that incidence of the disease has risen by an alarming 11% over the recent years, and a further doubling of new cases is predicted in the next 25 years.



**TABLE II**

Optimal conditions of enzyme reactions

glucose	histamine
GOx 0.48U/ml	DAO 0.8U/ml
HRP 0.2U/ml	HRP 0.2U/ml
ABTS 30mM	ABTS 30mM
Phosphate buffer 100mM	Phosphate buffer 100mM
pH 7.0 / 25°C	pH 7.0 / 37°C



**TABLE III**

Enzyme kinetic parameters

(a) glucose oxidase (GOx) catalysis reaction

650nm	$V_{max}$	$K_m$ (mM)	$V_{max}/K_m$
spectrophotometer	$2.2 \pm 0.03$	$7.2 \pm 0.2$	0.31
sensor system	$1.6 \pm 0.07$	$4.9 \pm 0.5$	0.33

(b) diamine oxidase (DAO) catalysis reaction

430 nm	$V_{max}$	$K_m$ ( $\mu$ M)	$K_{cat}$
spectrophotometer	$0.016 \pm 0.0014$	$160 \pm 19.7$	0.0001
sensor system	$0.004 \pm 0.0002$	$125 \pm 3.21$	0.00003

Enzyme kinetic analysis results of glucose oxidase and diamine oxidase observed in our assembled biosensor system approached to that obtained from UV/Vis spectrophotometer.

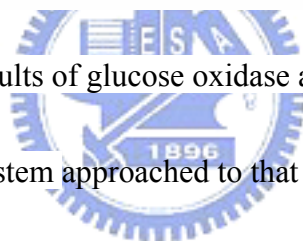


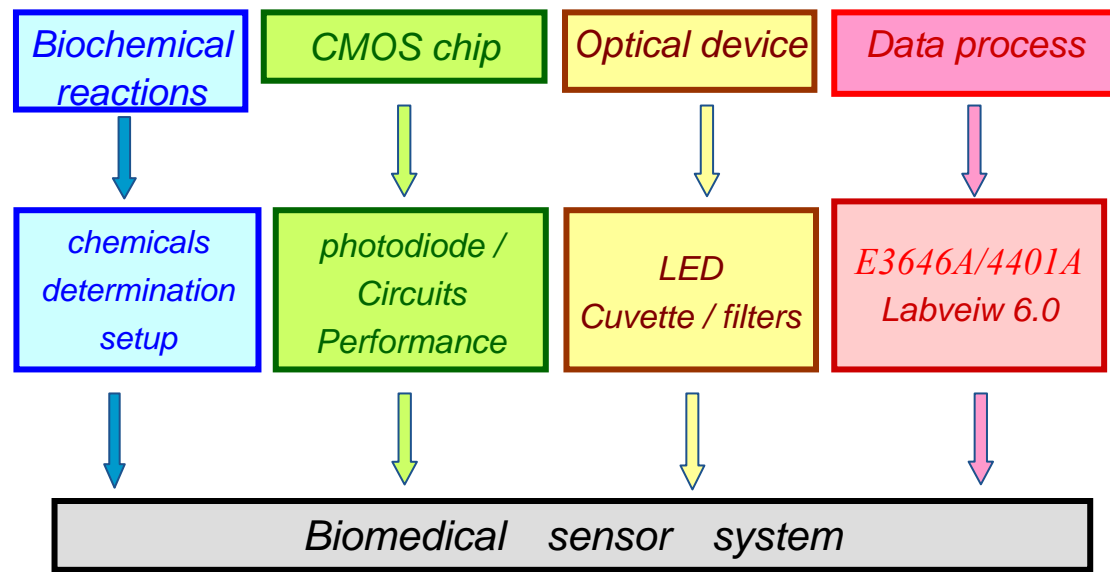
**TABLE IV**

The features of spectrophotometer and the assembled biosensing system

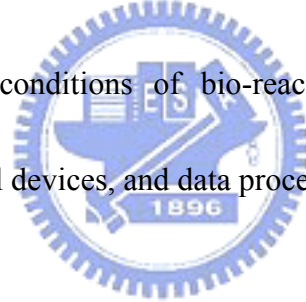
	Spectrophotometer	Our biosensing system
Features	<ol style="list-style-type: none"><li>1. Large volume</li><li>2. High cost (more than 300 thousand NTD)</li><li>3. High sensitivity (2.5 A650/min per <math>\mu\text{M}</math> of glucose)</li></ol>	<ol style="list-style-type: none"><li>1. Small volume</li><li>2. Low cost (less than 15 thousand NTD)</li><li>3. High sensitivity (3.0 A650/min per <math>\mu\text{M}</math> of glucose)</li></ol>



## Figures



**Fig. 1. The flowchart of research.** A biomedical sensor system assembled four main components: optimal conditions of bio-reactions, CMOS chip consist of photodiode and circuit, optical devices, and data process software.



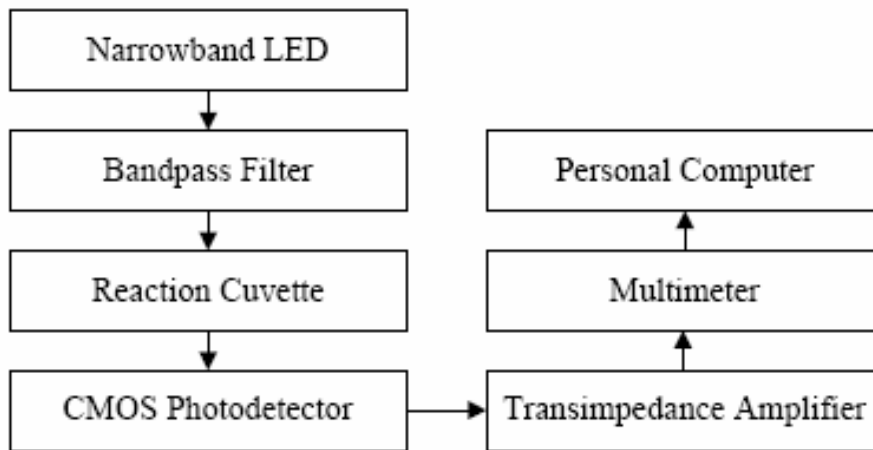
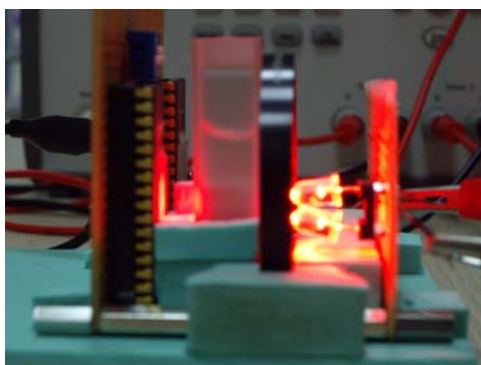
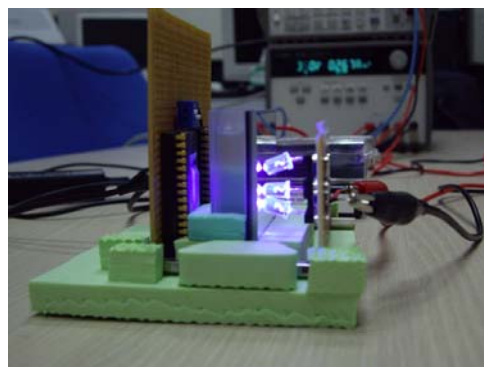


**Fig. 2. The flowchart of CMOS optical biosensing system.** A narrowband LED was used as the light source, and a bandpass filter allowed the light of a specific wavelength to travel through the cuvette, in which the light was modulated by the biochemical materials. The light, after passing through the cuvette, was detected by the CMOS biochip. The CMOS photo detector converted the modulated optical signals into current signals, and then the transimpedance amplifier (TIA) converted them into voltage signals. Finally, the signals were recorded by a multimeter and processed by personal computer.



650 nm system



430 nm system



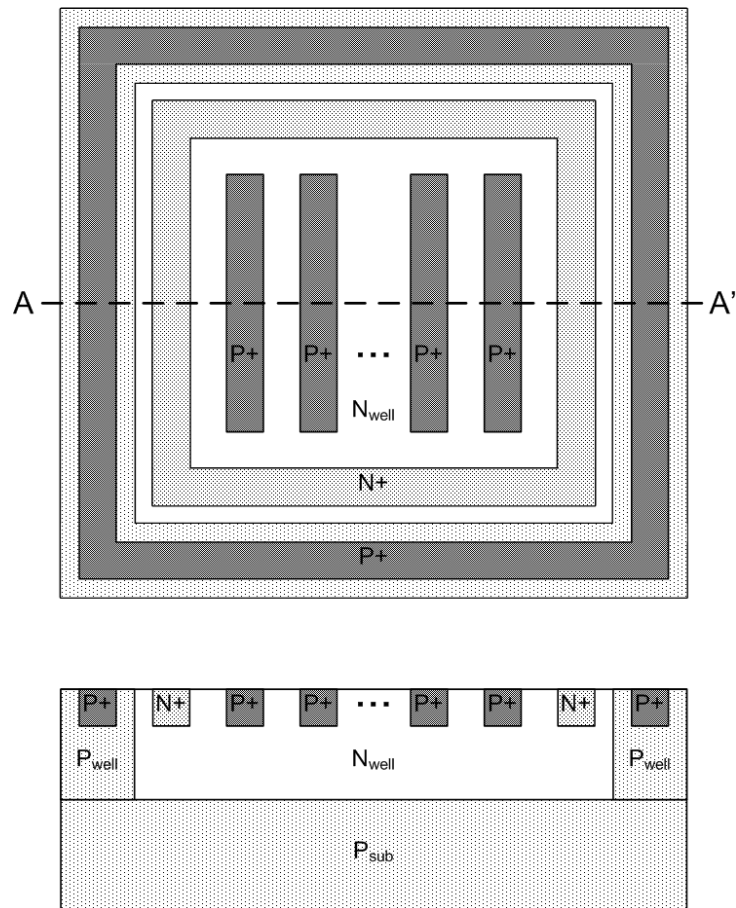


**Fig. 3. Top view and cross section of P+/N well finger photodiode.** Each P+ stripe is 1 $\mu\text{m}$  wide with 4  $\mu\text{m}$  spacing, and the total area of this finger photodiode is 100  $\mu\text{m}$   $\times$  100  $\mu\text{m}$ . The photodiode is surrounded by double guard rings to keep the substrate noise off; the P+ guard ring is connected to ground, and the N+ guard ring is connected to a high potential. Photodiode with finger structure (p+-n well) is designed by Yu-Wei Chang who is a Ph.D. student of the department of electronic engineering at NCTU.

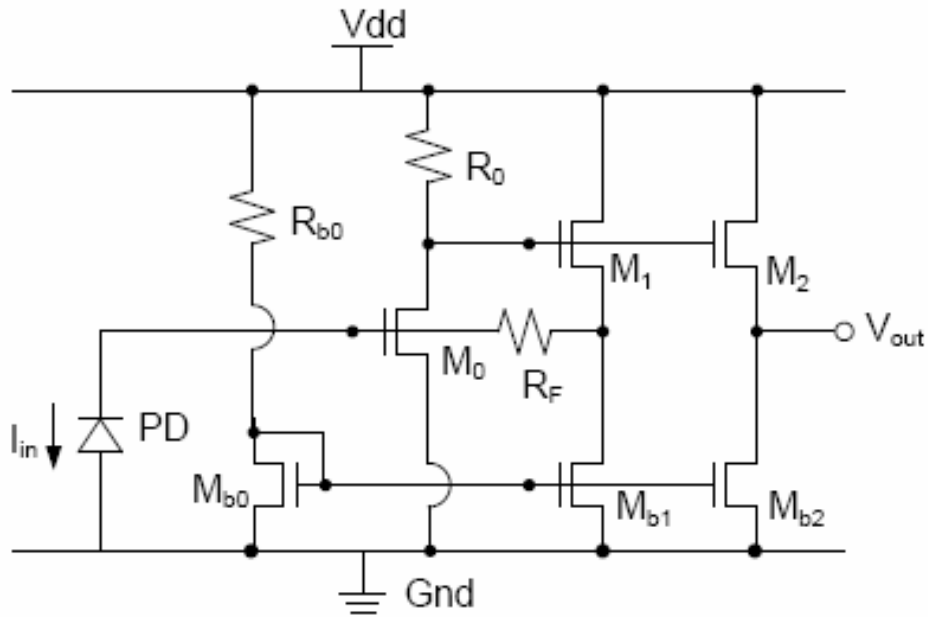


**Fig. 4. The configuration of subsequent circuits.** The subsequent circuits include

a current source, current mirrors, a TIA, and output buffers. The TIA consists of a common-source stage ( $M_0$ ), two source followers ( $M_1$  and  $M_2$ ), and an external feedback resistance ( $R_F$ ).  $M_1$  serves in the feedback loop to isolate  $R_0$  from the loading effect, and  $M_2$  drives the load capacitance to alleviate the stability issue.

Current amplifier, TIA circuit with variable resistance are designed by Yu-Wei Chang who is a Ph.D. student of the department of electronic engineering at NCTU.

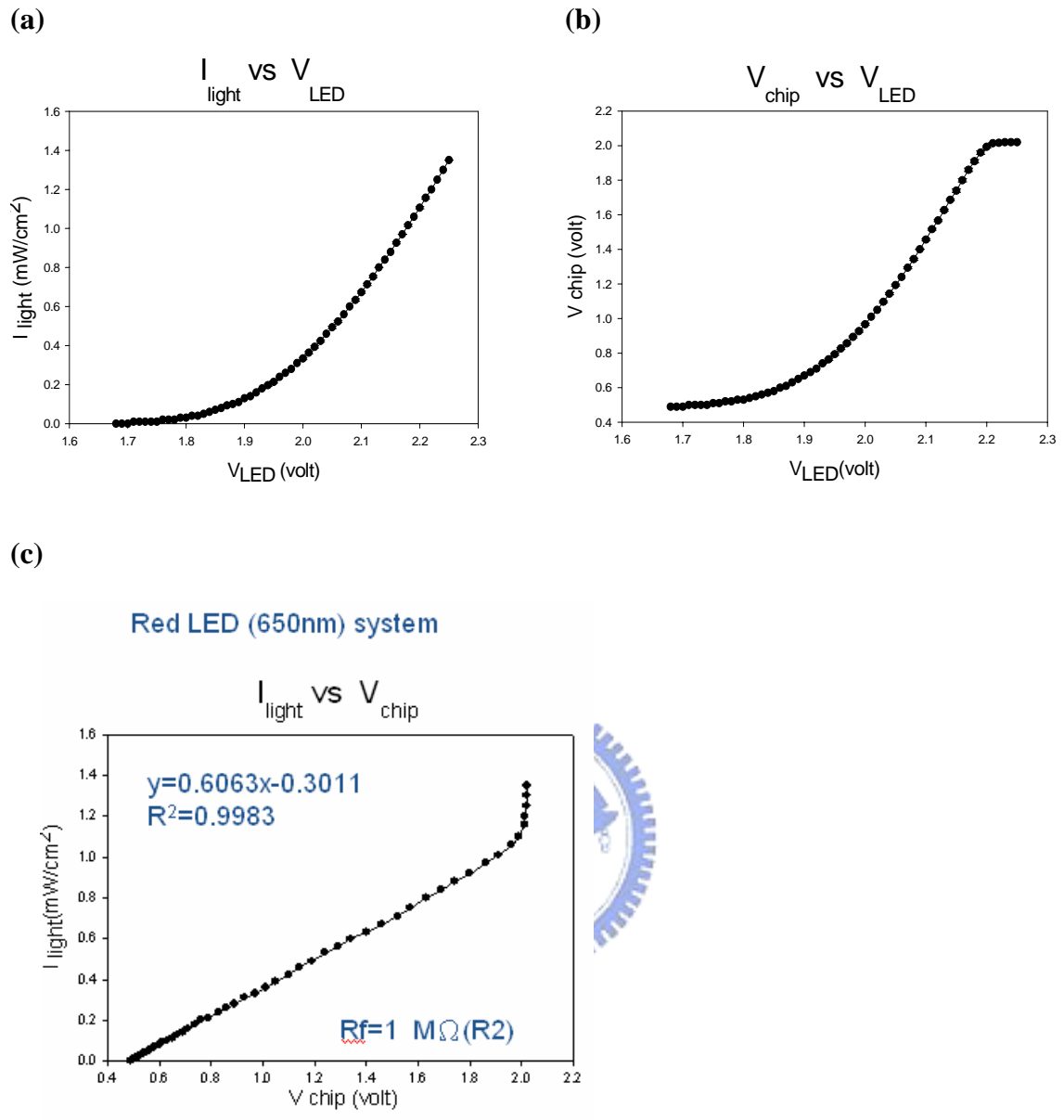
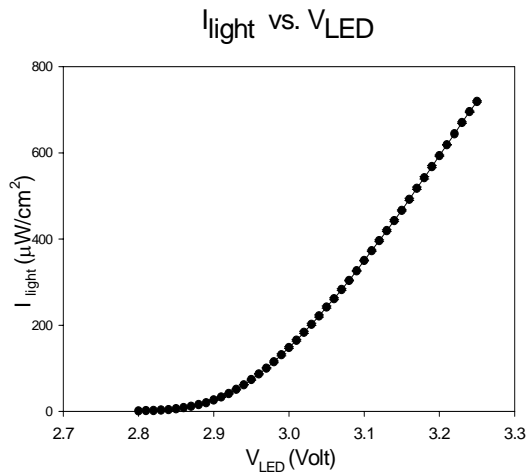
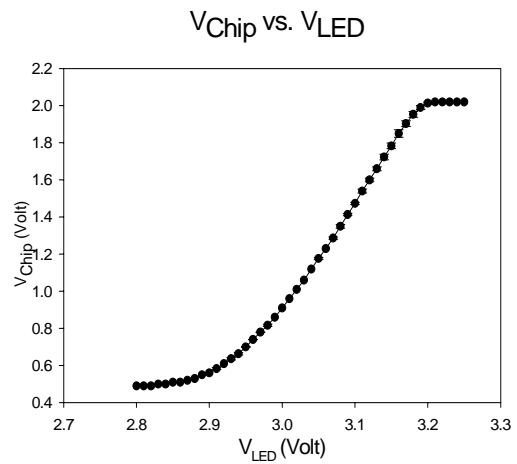


**Fig. 5.** (a)The curve of LED (650nm) input voltage versus light intensity (b)The curve of LED (650nm) input voltages versus CMOS chip output voltage (c). The curve of light intensity versus CMOS chip output voltage. With a 3.0 V power supply, the lower bound and upper bound of the output voltage are 0.49 V and 2.02 V, respectively.

(d)



(e)



(f)

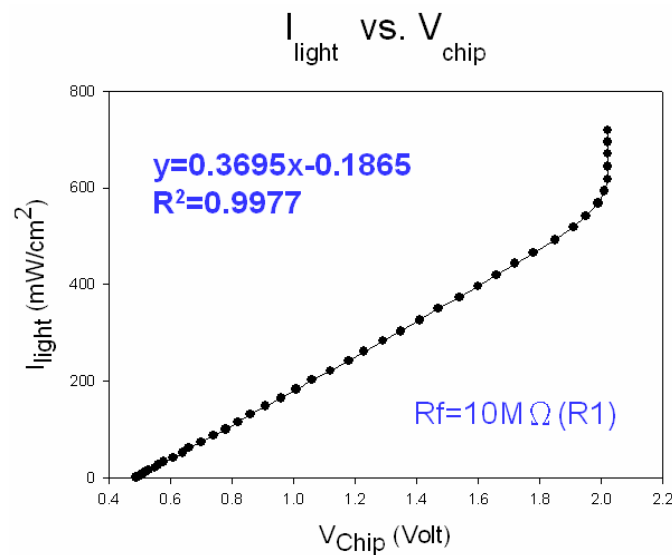


**Fig. 5.** (d)The curve of LED (430nm) input voltage versus light intensity. (e)The curve of LED (430nm) input voltages versus CMOS chip output voltage (f). The curve of light intensity versus CMOS chip output voltage at 430nm. With a 3.0 V power supply, the lower bound and upper bound of the output voltage are 0.49 V and 2.02 V, separately.

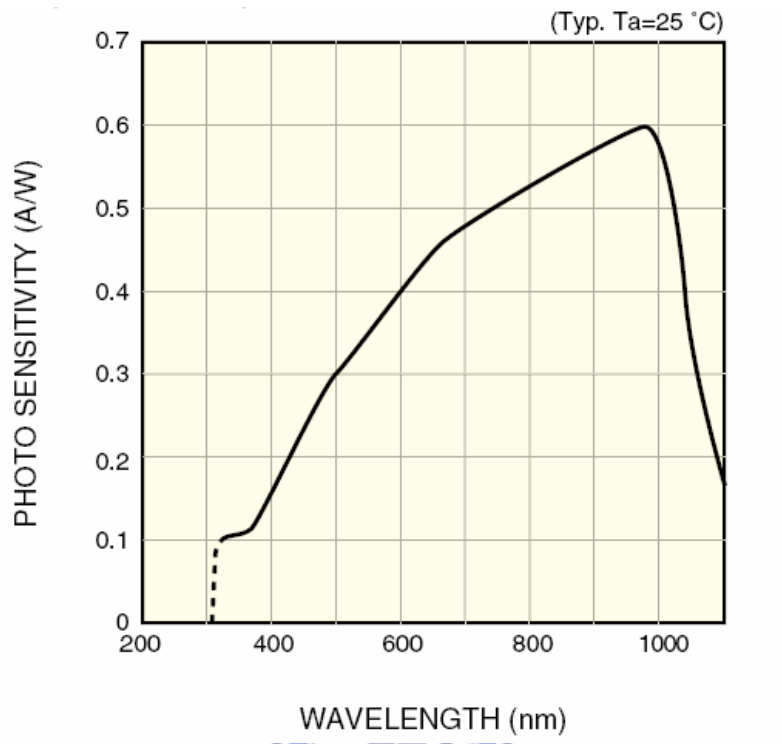


**Fig. 6. CMOS photodiode light absorption spectrum.** It illustrates the absorption peak of photodiode between 400 and 1000 nm, and it is obvious that the maximum absorption peak of photodiode within the visible light ranges between 600 and 700nm.

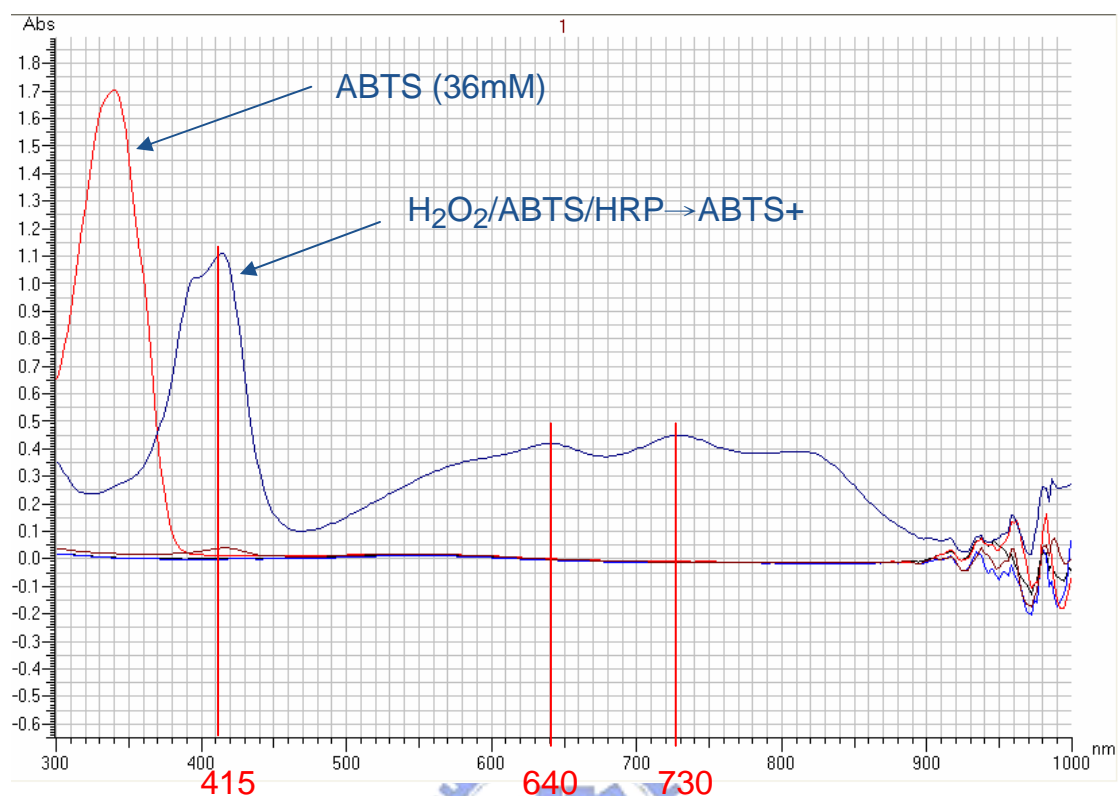


**Fig. 7. The absorption spectrum (300~1000nm) of ABTS / H<sub>2</sub>O<sub>2</sub> colorimetry reaction.** The scan parameters of UV-3310 are as follows: start wavelength is 1000 nm, end wavelength is 300 nm, delay time is 120 sec, scan speed is 300 nm/min and slit is 2 nm. Reaction condition is: 25°C, pH 7.0, 100 mM Phosphate buffer, 30 mM ABTS, 0.2 mM H<sub>2</sub>O<sub>2</sub> and 0.2 unit/ml HRP. The absorption wavelength of the product of reaction, ABTS<sup>•+</sup> has three absorption peaks at 415 nm, 640 nm and 730 nm, separately.

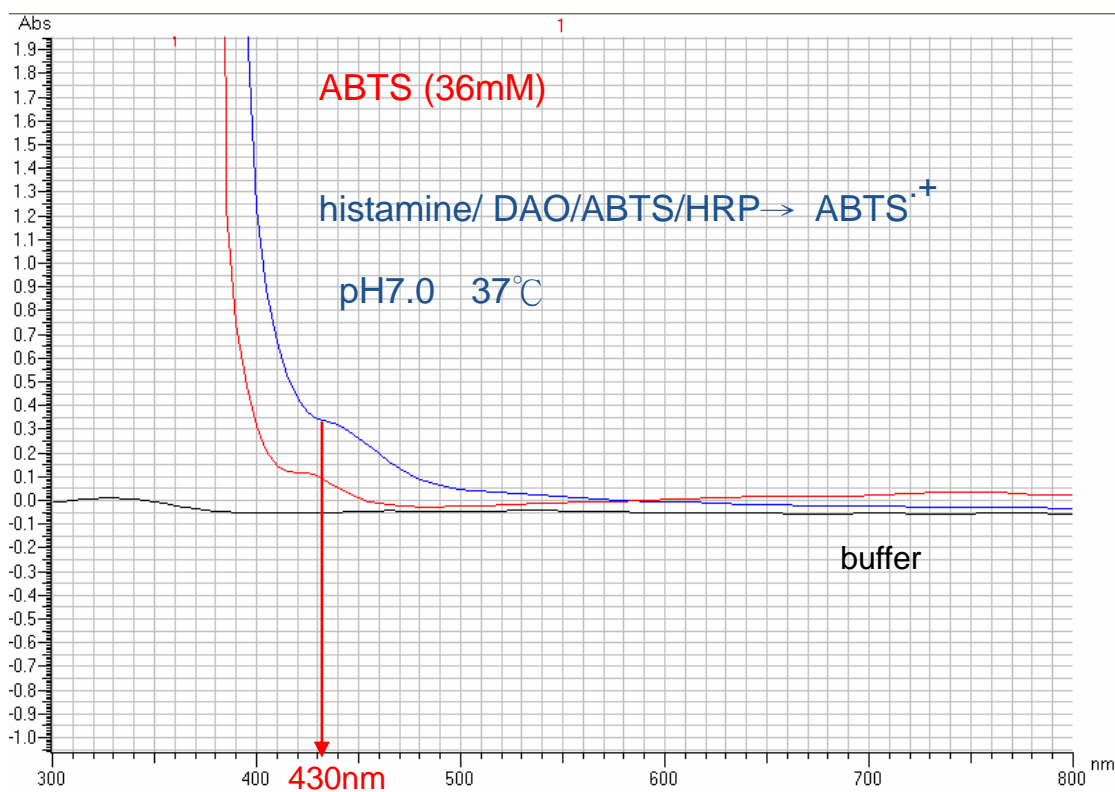


**Fig. 8.** The absorption spectrum (300~1000nm) of the coupled enzyme reactions catalyzing histamine. The scan parameters of UV-3310 are as follows: start wavelength is 1000 nm, end wavelength is 300 nm, delay time is 120 sec, scan speed is 300 nm/min and slit is 2 nm. Reaction conditions: 37°C, pH 7.0, 100 mM Phosphate buffer, 30 mM ABTS, 0.4 mM histamine, 0.48 unit/ml DAO and 0.2 unit/ml HRP. The product of coupled enzyme reactions catalyzing histamine had only one light absorbance peak at 430 nm.

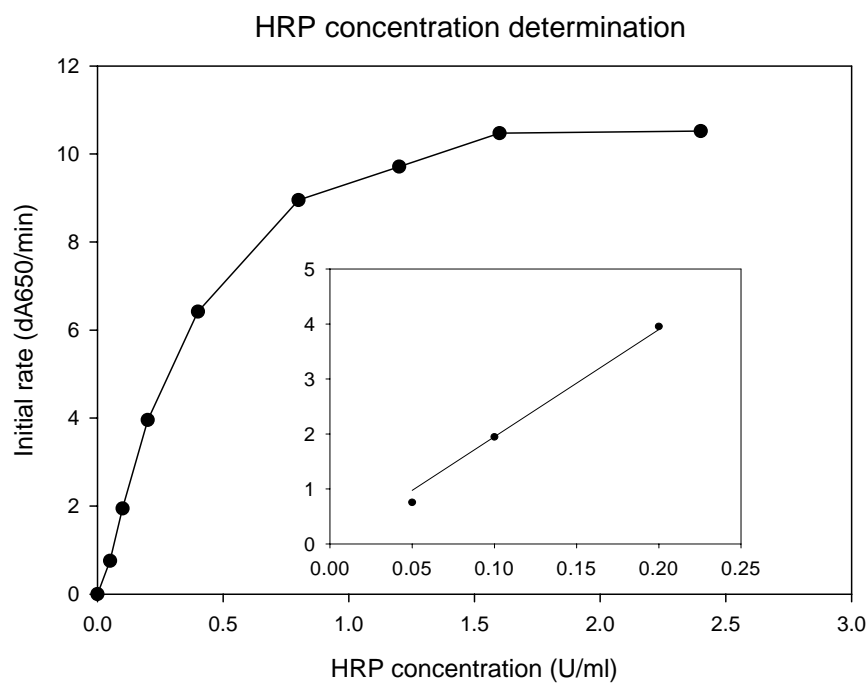


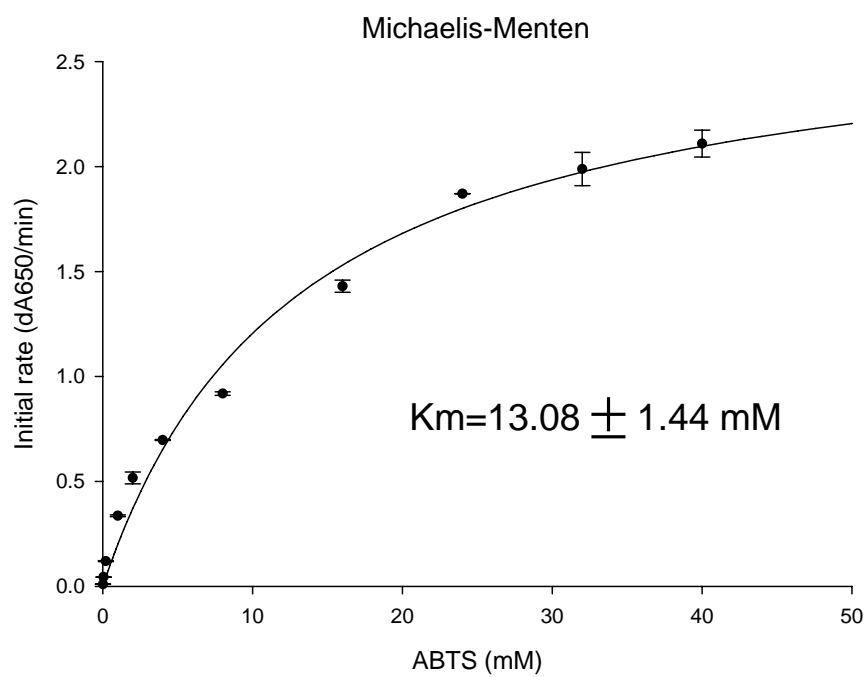
**Fig. 9. The curve of initial rate versus the different HRP concentration** Reaction

conditions: ABTS 30 mM,  $H_2O_2$  400  $\mu$ M, Phosphate buffer 100mM, pH 7.0 and 25°C .

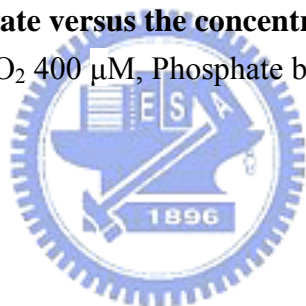
There is a linear range of HRP between 0.05 to 0.2 U/ml; therefore, we choose 0.2

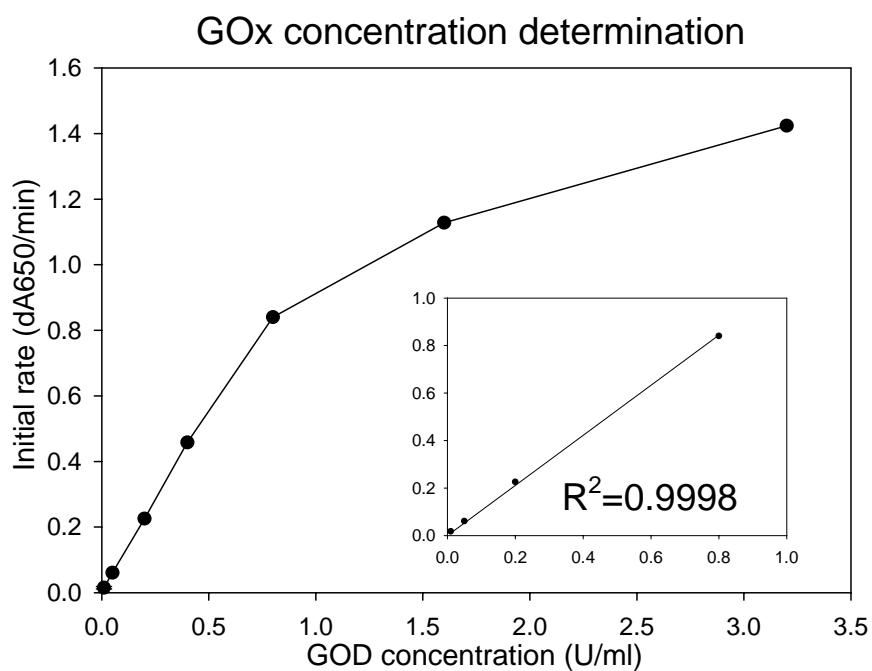
U/ml of HRP to catalyze in the ABTS/ $H_2O_2$  colorimetry system.





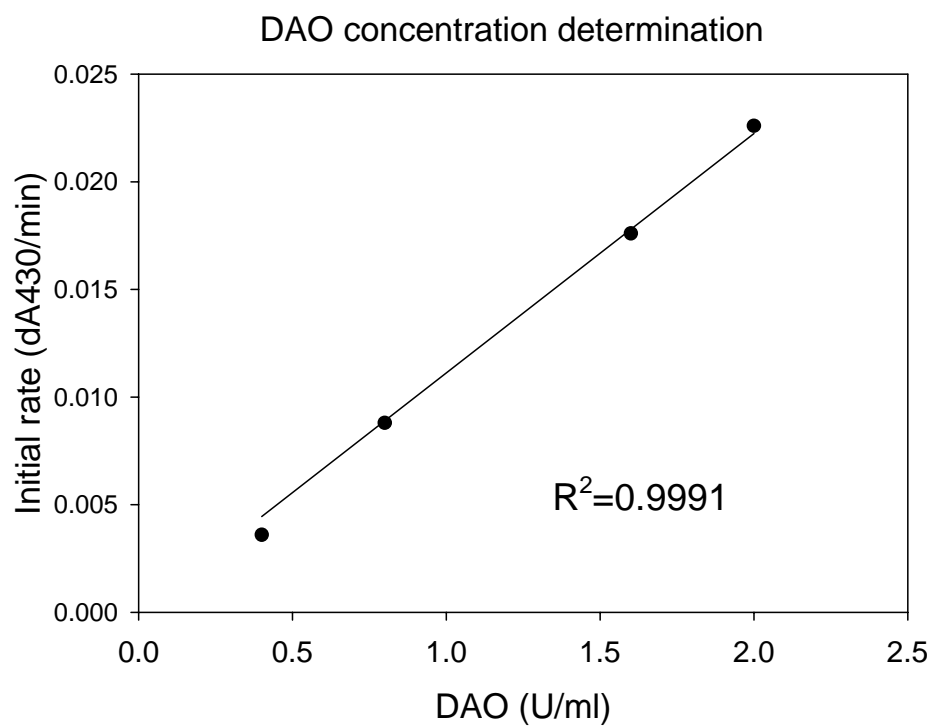
**Fig. 10. The curve of initial rate versus the concentration of ABTS.** Reaction conditions : HRP 0.2U/ml,  $\text{H}_2\text{O}_2$  400  $\mu\text{M}$ , Phosphate buffer 100mM, pH 7.0 and 25°C.





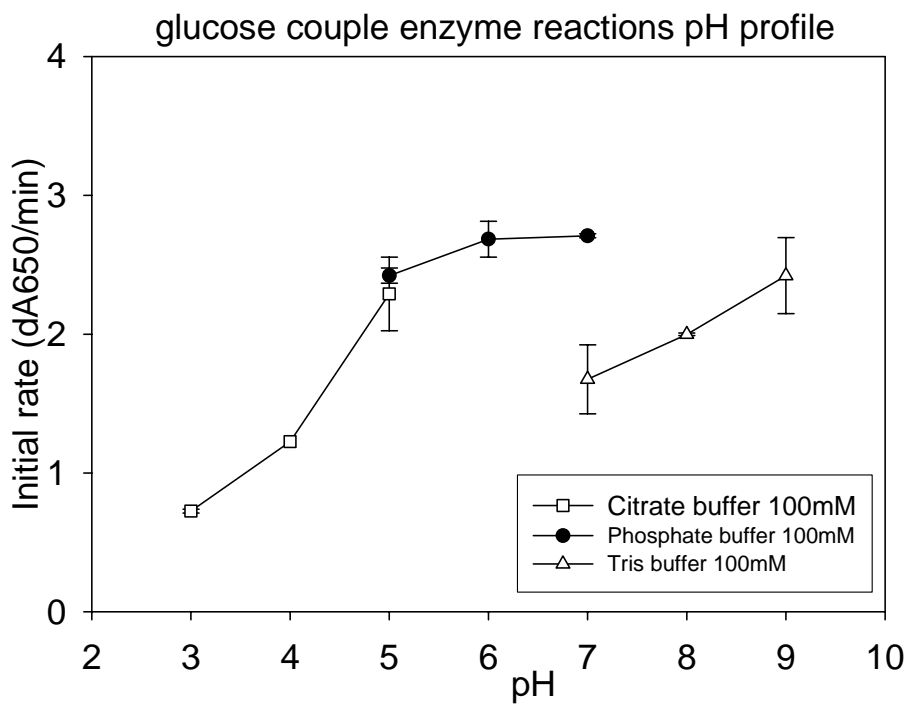
**Fig. 11. The curve of initial rate versus the different GOx concentration**

Reaction conditions: glucose 100mM, HRP 0.2U/ml, ABTS 30mM, phosphate buffer 100mM, pH 7.0 and 25°C. The linear range of glucose oxidase ranged from 0.01 to 0.8 U/ml.

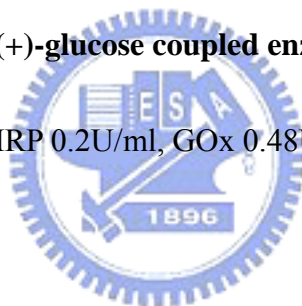


**Fig. 12. The curve of initial rate versus the different DAO concentration**

Reaction conditions: histamine 2mM, HRP 0.2U/ml, ABTS 30mM, phosphate buffer 100mM, pH 7.0 and 37°C. The linear range of diamine oxidase ranged from 0.4 to 2 U/ml



**Fig. 13. The pH profile of D-(+)-glucose coupled enzyme reactions.** Reaction conditions: glucose 100mM, HRP 0.2U/ml, GOx 0.48U/ml, ABTS 30mM, and 25°C.



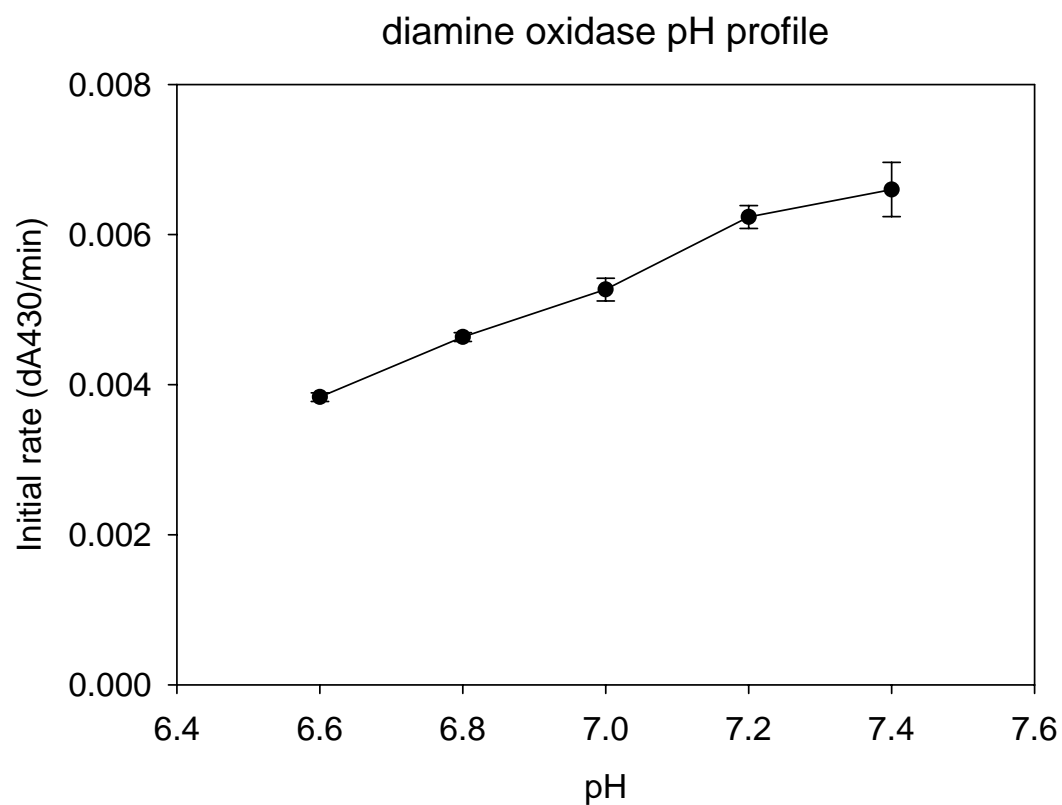


**Fig. 14. The pH profile of histamine coupled enzyme reactions.** Reaction conditions: histamine 400 $\mu$ M, HRP 0.2U/ml, DAO 0.8U/ml, ABTS 30mM and 37 $^{\circ}$ C.

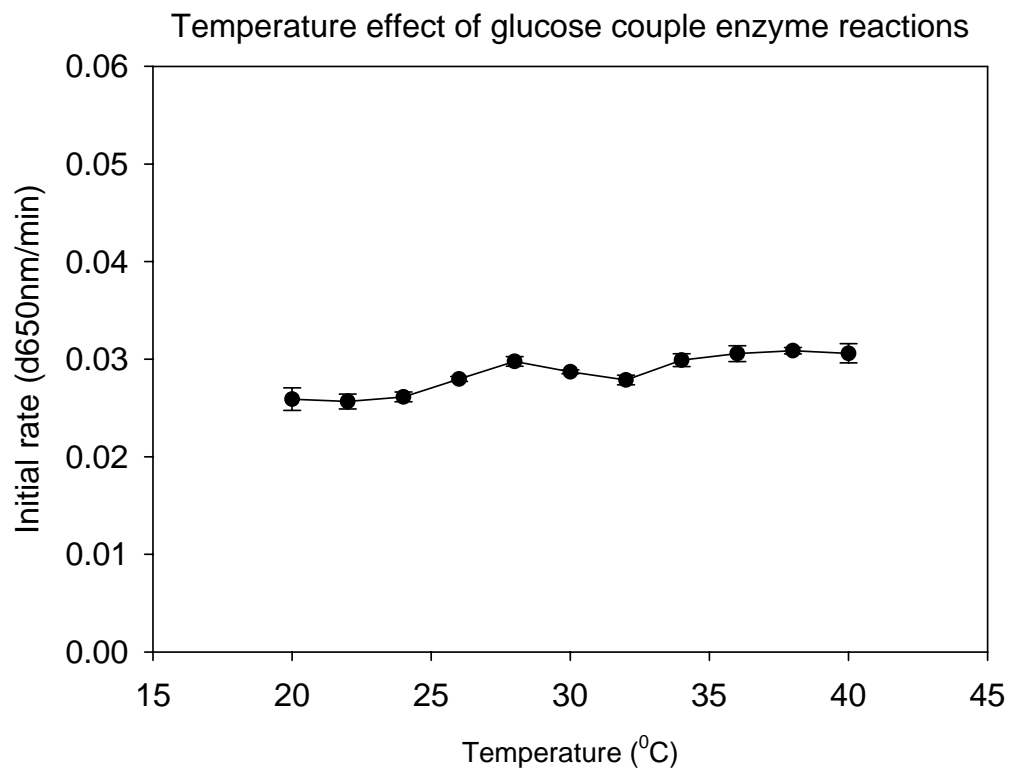


**Fig. 15. The temperature effect of D-(+)-glucose coupled enzyme reactions.**

Reaction conditions: glucose 100mM, HRP 0.2U/ml, GOx 0.48U/ml, ABTS 30mM, phosphate buffer 100mM and pH 7.0.

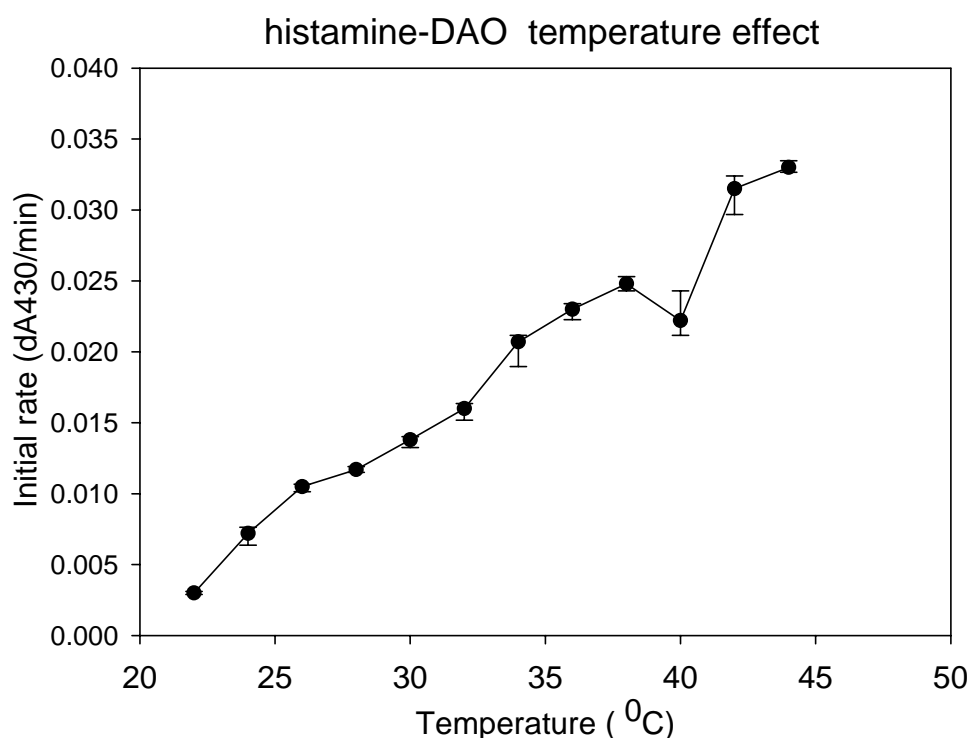


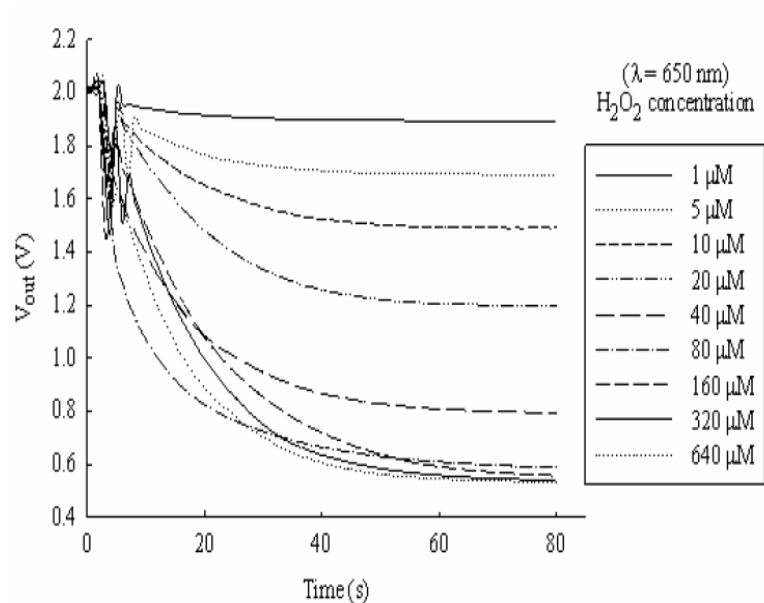
**Fig. 16. The temperature effect of histamine coupled enzyme reactions.** Reaction

conditions: histamine 2mM, HRP 0.2U/ml, DAO 0.8U/ml, ABTS 30mM, phosphate

buffer 100mM and pH 7.0.



(a). 650 nm system



(b). 430 nm system

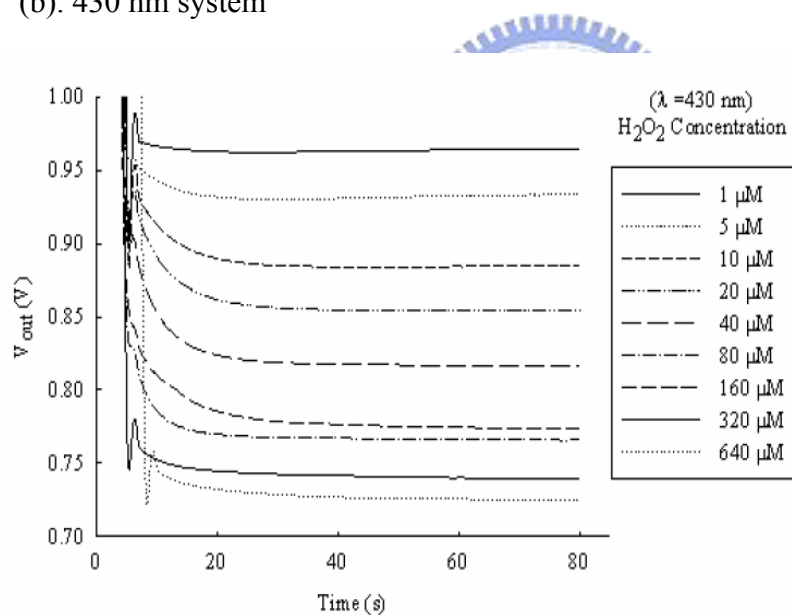


**Fig. 17. The CMOS chip output voltage at different hydrogen dioxide**

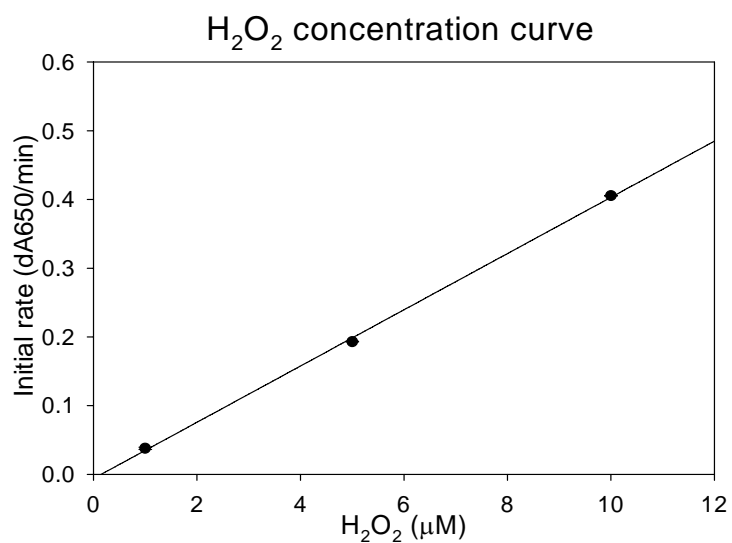
**concentrations in the 650 nm and 430 nm system. Reaction conditions: (a)**

HRP 0.2U/ml, ABTS 30mM, Phosphate 100mM, pH 7.0 and 37°C. (b) HRP

0.2U/ml, ABTS 30mM, Phosphate 100mM, pH 7.0 and 25°C.



(a). 650 nm bio-sensing system



(b). 650 nm UV/Vis spectrophotometer

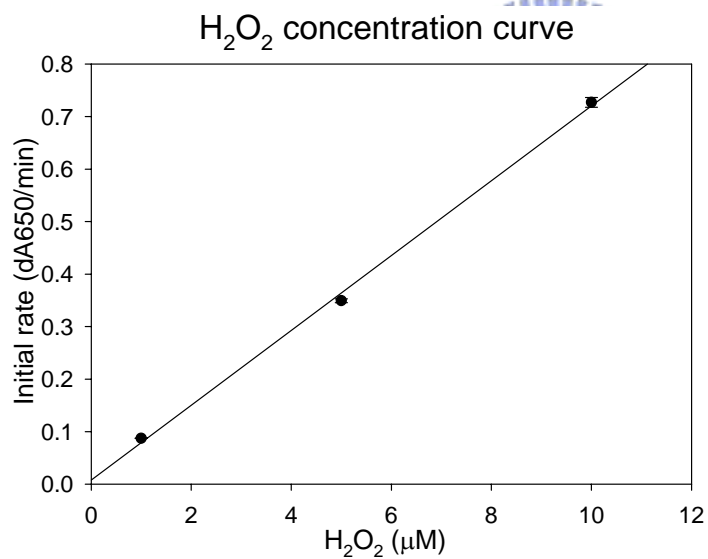
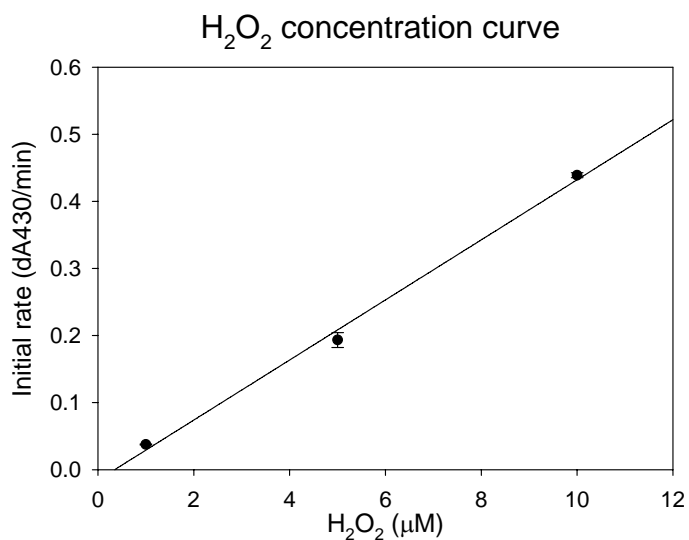


**Fig. 18. Hydrogen dioxide detection limit in the 650 nm system.** Reaction

conditions (both on (a) and (b)): HRP 0.2U/ml, ABTS 30mM, Phosphate 100mM, pH

7.0 and 25°C. (a) The detection limit is 1 μM. (b) The detection limit is 1 μM.

(a). 430 nm bio-sensing system



(b). 430 nm UV/Vis spectrophotometer

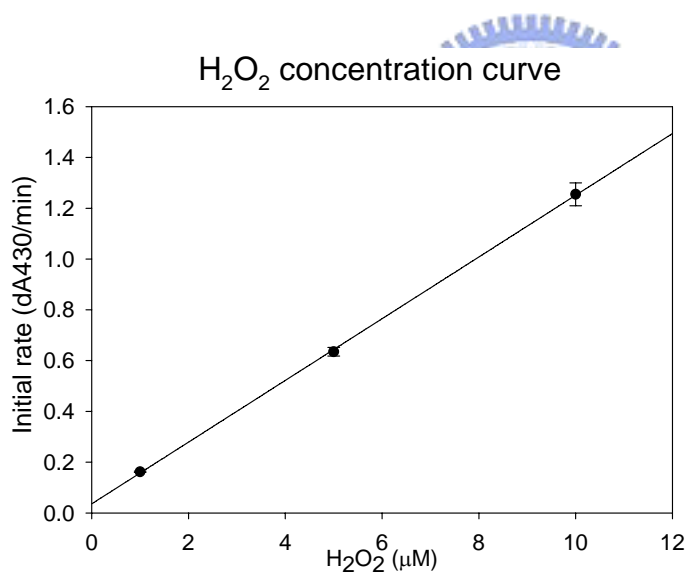
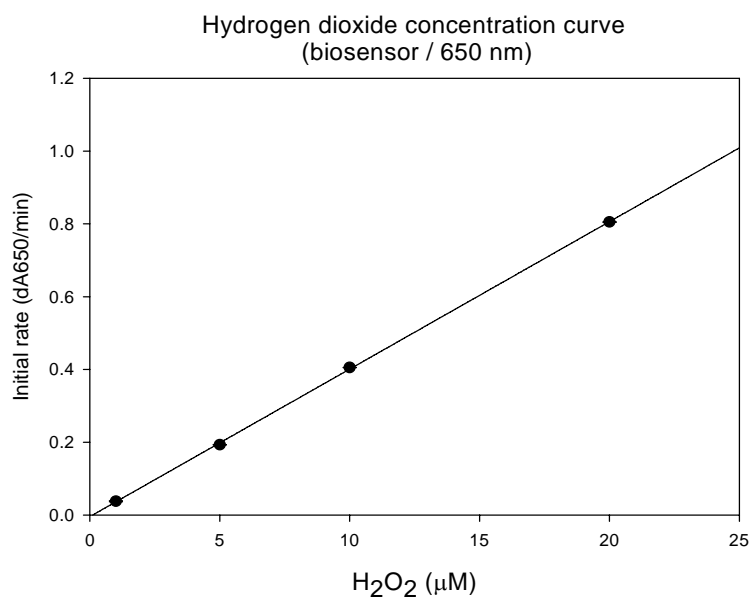


**Fig. 19. Hydrogen dioxide detection limit in the 430 nm system.** Reaction

conditions (both on (a) and (b)): HRP 0.2U/ml, ABTS 30mM, Phosphate 100mM,

pH 7.0 and 37°C. (a) The detection limit is 1  $\mu M$ . (b) The detection limit is 1  $\mu M$ .

**(a). 650 nm bio-sensing system**



**(b). 650 nm UV/Vis spectrophotometer**

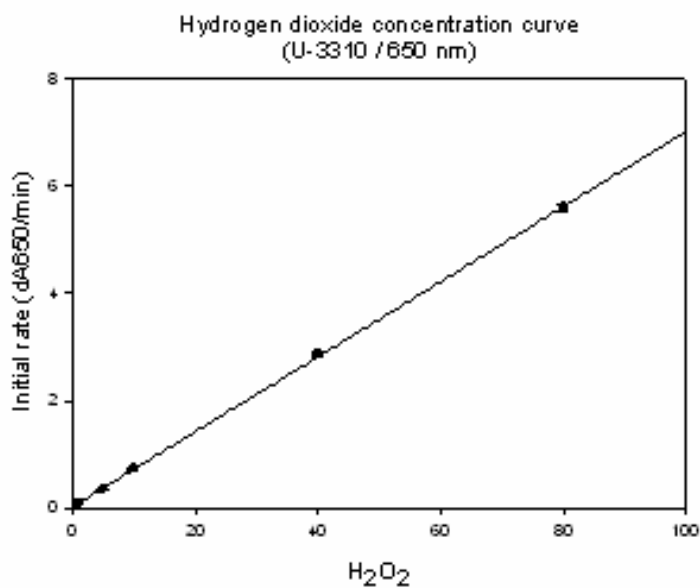
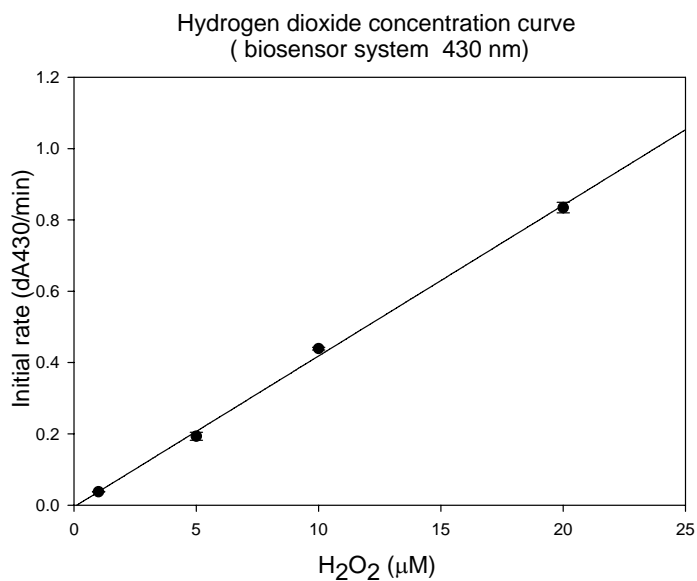


**Fig. 20. Hydrogen dioxide linear detection range in the 650 nm system.** Reaction conditions (both on (a) and (b)): HRP 0.2U/ml , ABTS 30mM, Phosphate 100mM, pH 7.0 and 25°C . (a) Linear detection range : 1 ~ 20μM. (b) Linear detection range : 1 ~ 80 μM.

**(a). 430 nm bio-sensing system**



**(b). 430 nm UV/Vis spectrophotometer**

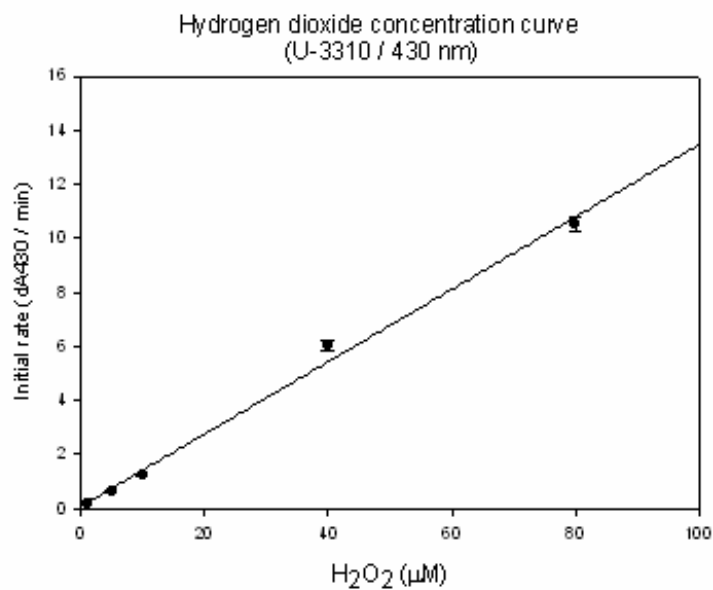
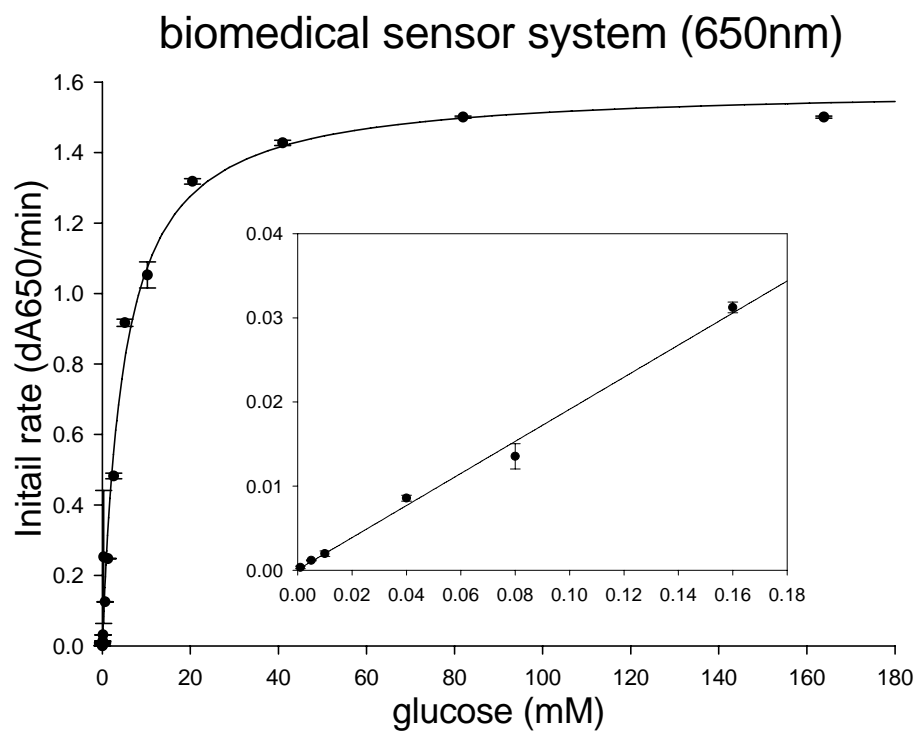
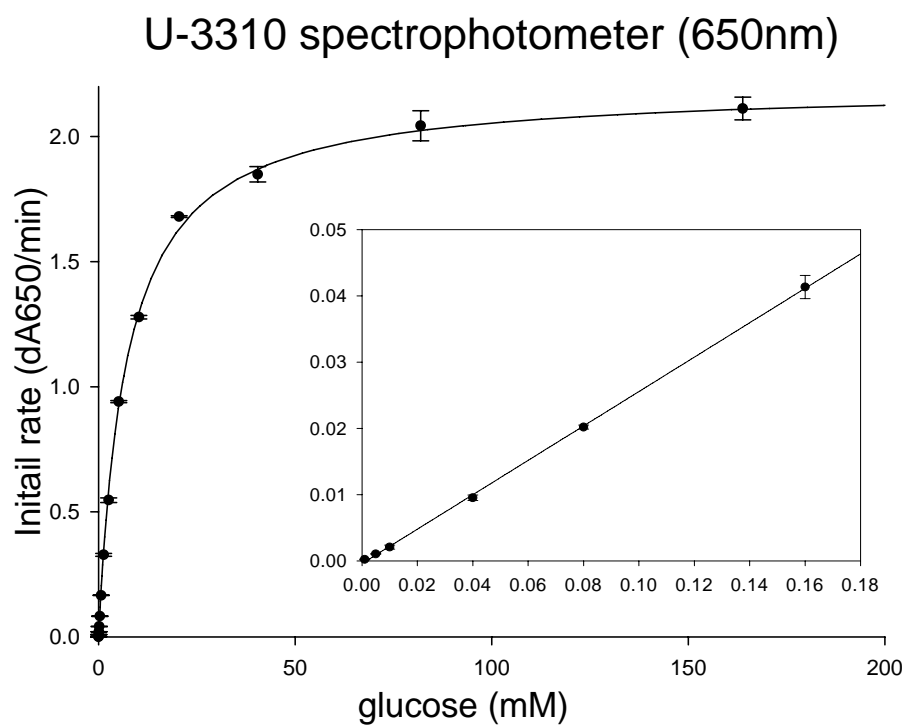


**Fig. 21. Hydrogen dioxide linear detection range in the 430 nm system.** Reaction conditions (both on (a) and (b)):HRP 0.2U/ml, ABTS 30mM, Phosphate 100mM, pH 7.0 and 37°C . (a) Linear detection range : 1 ~ 20μM. (b) Linear detection range : 1 ~ 80 μM.

(a)



(b)



(c)

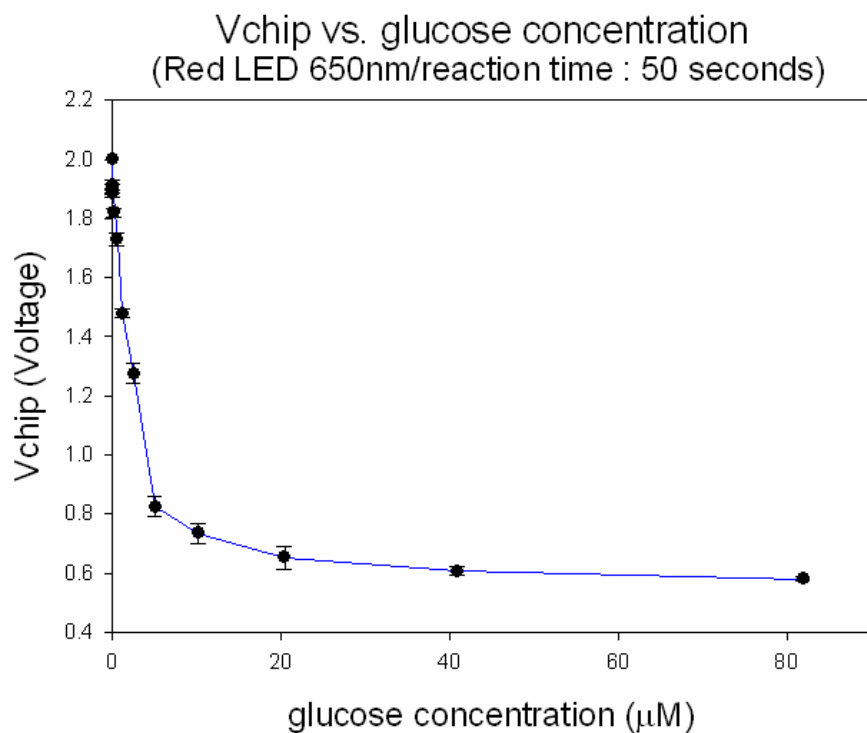
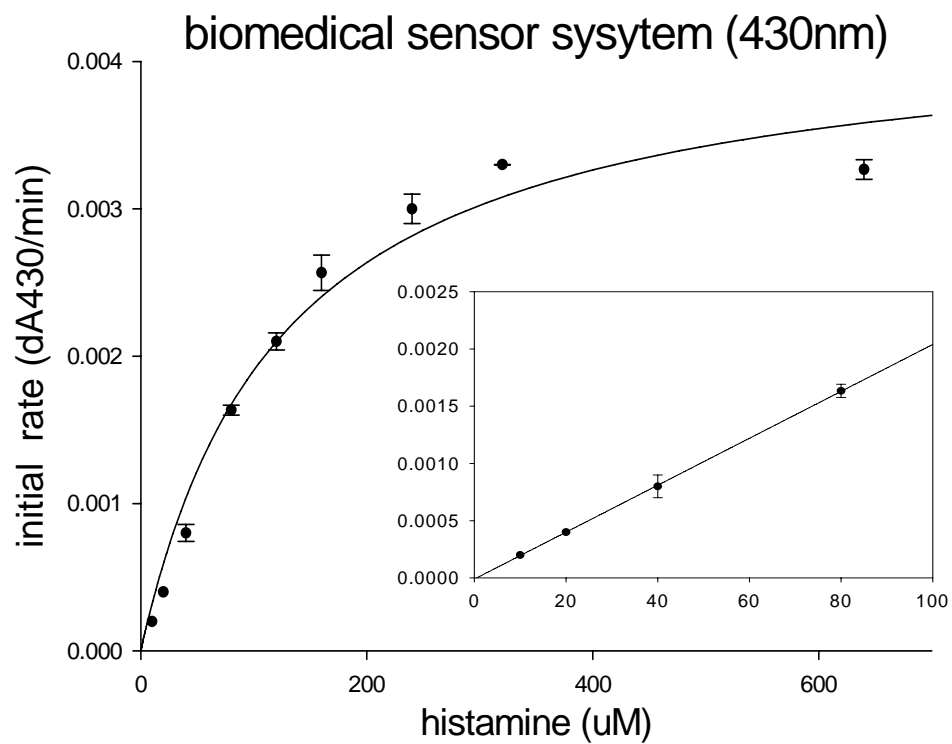
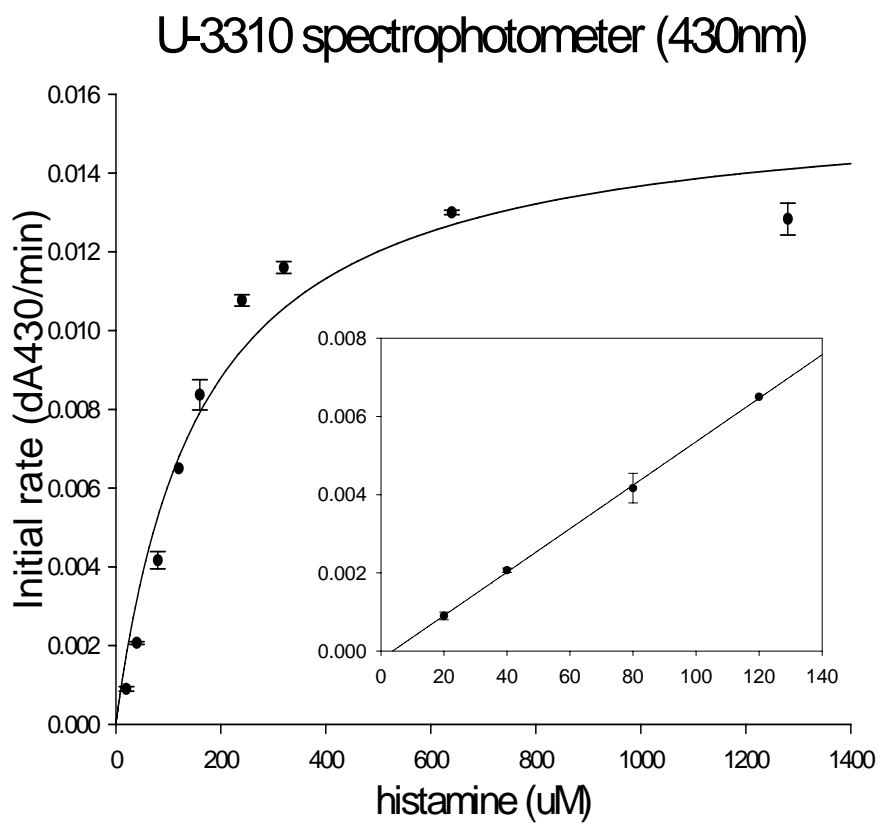


**Fig. 22. Enzyme kinetic analysis curve of glucose oxidase.** (a) on our assembled biosensor system. (b) on UV/Vis spectrophotometer (UV-3310). (c) CMOS chip output voltage at different glucose concentration. Reaction conditions (on (a), (b) and (c)): HRP 0.2U/ml, GOx 0.48U/ml, ABTS 30mM, Phosphate buffer 100mM, pH 7.0 and 25°C. Input voltage of CMOS chip is 3.0 V, and input voltage of LED is 2.25V. The detection limit are 1  $\mu\text{M}$  on both (a) and (b). The liner detection ranges of our assembled biosensing system ranged from 1  $\mu\text{M}$  to 5 mM on both (a) and (b).

(a)



(b)



(c)

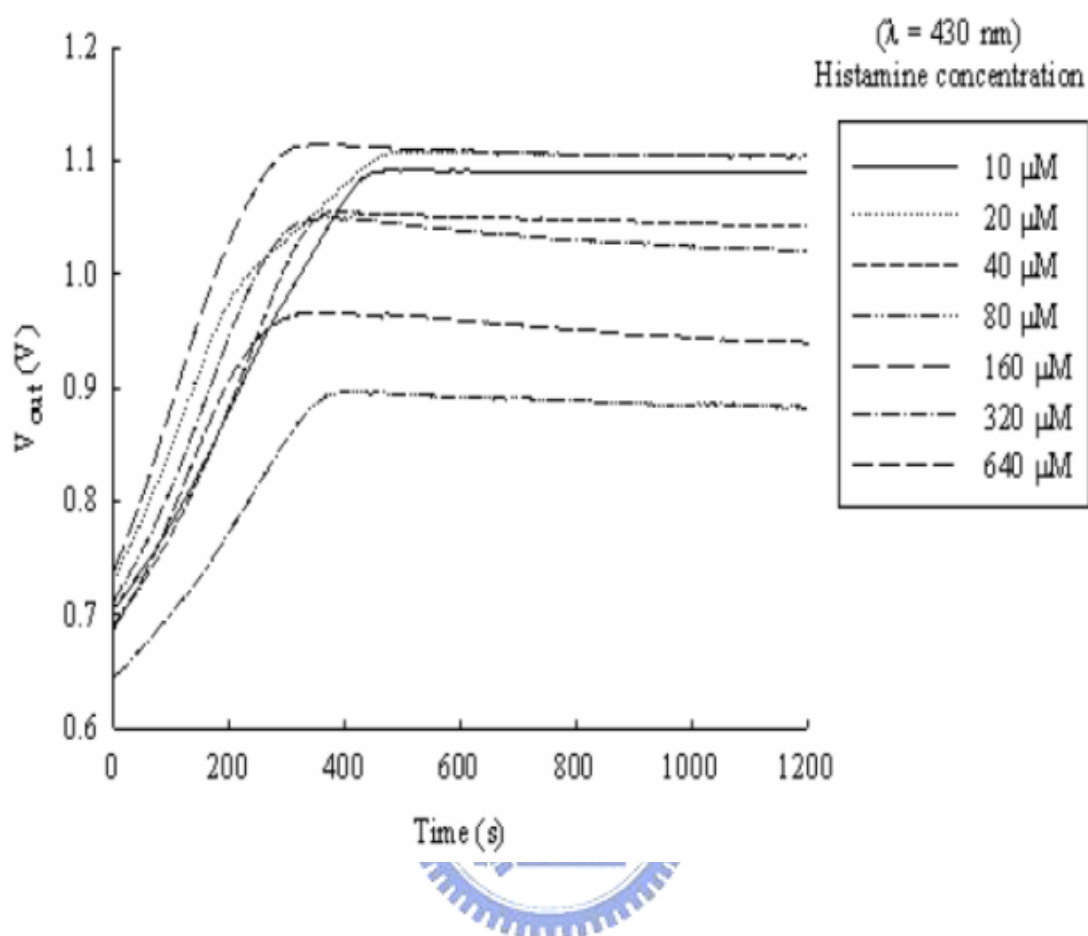


**Fig. 23. Enzyme kinetic analysis curve of diamine oxidase.** (a) on our assembled biosensor system. (b) on UV/Vis spectrophotometer (UV-3310). (c) CMOS chip output voltage at different histamine concentration. Reaction conditions (on (a), (b) and (c)): HRP 0.2U/ml, DAO 0.8U/ml, ABTS 30mM, Phosphate buffer 100mM, pH 7.0 and 37°C. Input voltage of CMOS chip is 3.0 V and input voltage of LED is 3.5V. The detection limit is 10  $\mu\text{M}$  on (a) and it is 20  $\mu\text{M}$  on (b). The liner detection ranges of our assembled biosensing system range from 10  $\mu\text{M}$  to 80  $\mu\text{M}$  on (a) and 20  $\mu\text{M}$  to 120  $\mu\text{M}$  on (b).